

**Advanced dynamic simulation of different pumping
methods in an AC-chilled water system**

Wilhelm Gustafsson



Master's thesis in Thermal and Flow Engineering

Supervisors Henrik Saxén and Tero Mäki-Jouppila

Thermal and Flow Engineering Laboratory
Faculty of Science and Engineering
Åbo Akademi University

Åbo, 2018

Acknowledgments

I would like to thank Professor Henrik Saxén at Åbo Akademi University for all his feedback and help in the thesis process. I also want to thank Meyer Turku and Kari Sillanpää for the opportunity to write this thesis. Also, a huge thank you to the personnel at Meyer Turku, especially Tero Mäki-Jouppila for supervising and helping me with the thesis and the rest of the Energy Efficiency team, Anniina Ukkonen, Mathias Pirttikangas and Vesa Lepistö, for helping me with the software and data used.

Last huge thanks for the support and help from Veera, my friends and family.

Åbo, November 2018

Wilhelm Gustafsson

Abstract

The International Maritime Organization has introduced stricter energy efficiency demands to compel ship builders to further reduce emissions on, e.g., cruise ships. Heating, ventilation and air conditioning (HVAC) represent approximately a third of the power consumption of the cruise ship hotel, which makes it an interesting target for improvements in energy efficiency.

Older cruise ships have no way to control the pumping in the AC-chilled water system. The prices on variable speed drives have recently dropped, making it profitable to reduce pumping power. Driving the system with a constant pressure difference instead of a constant flow could cut down on pumping power significantly.

The goal of this thesis was to study the AC-chilled water system and construct a simulation model that could be used to validate the savings of different pumping methods. The model was to be well documented and modifiable for possible future use.

A simulation model was built in Apros dynamic simulation software. The model was successfully validated using data from an existing ship. The different pumping methods were simulated and the results were compared and analyzed. The simulation results showed that the variable primary flow method would save considerable pumping power.

Key words: cruise ship, dynamic simulation, energy efficiency, pumping method, chilled water system, air conditioning, Apros.

Contents

Acknowledgments	ii
Abstract	iii
Contents	iv
1. Introduction.....	1
1.1. Problem	1
1.2. Objective.....	1
2. Background.....	3
2.1. Energy Efficiency Design Index	4
2.2. Customers and passenger requirements	5
2.3. Literature review	7
2.4. Savings potential	8
3. Air conditioning theory.....	10
3.1. Air properties.....	10
3.2. AC chillers	12
3.2.1. Electric compressor chillers.....	12
3.2.2. Alternative chillers.....	15
3.3. Reheaters.....	18
3.4. Air handling units.....	19
3.5. Fan Coil Units.....	21
4. Pumping methods	23
4.1. Pump theory	23
4.2. Constant flow	24
4.3. Primary–secondary flow.....	25
4.4. Variable flow.....	26
4.5. Dedicated or manifold pumps.....	27
5. Simulation tool	29

5.1. Apros dynamic simulation tool.....	29
6. Model set up.....	32
6.1. Set point values	34
6.2. Automation control	34
6.3. Testing and optimizing the model.....	35
7. Validation.....	37
7.1. Validation results.....	40
7.2. Conclusion of validation	42
8. Simulations	44
8.1. Input data	44
8.2. Results	48
8.2.1. Constant flow	48
8.2.2. Primary–secondary flow.....	50
8.2.3. Primary flow	52
8.2.4. Comparing the results	53
9. Discussion	60
10. Conclusion	63
Svensk sammanfattning	65
References.....	68
Figures	73
Tables.....	75

1. Introduction

All industries - the tourist industry included - are under an increasing pressure to reduce their environmental impact and stop, or at least slow down, global warming. The cruise industry is rapidly growing, and the new-built ships have to be more energy efficient. Both owners and international organizations are demanding higher energy efficiency of the ships. As the environmental requirements are increasing, new ways to be more energy efficient are needed. This makes the need to save power an important aspect for all parts of the ship's technology.

Passengers are not willing to compromise the experiences on the cruises, even though the environmental impact has to be reduced. The reductions in the energy demand and emissions have to be met without sacrificing comfort or experience.

Air conditioning is a very important requirement in the hot and humid climates where luxury cruise ships are operating, both for passenger comfort and to keep the ship free from mold and rust. Air conditioning is responsible for a large part of the energy consumption onboard, and represents around a third of the cruise-ship hotel's demand (Meyer, 2018). This makes it a very interesting target to find major savings.

1.1. Problem

Cruise ships conventionally use a constant flow method of pumping chilled water to the air handling units and fan coil units. This results in wasted pumping energy since large quantities of water are pumped through the ship, even if a fraction of it would suffice.

It is always important to be able to verify and calculate the savings which new technology could contribute to, both for the ship yard and for the ship owner. An important tool for this is dynamic simulation software. To be able to simulate different scenarios and technologies, an accurate and flexible model has to be developed in the dynamic simulation environment.

1.2. Objective

The objective of this thesis is to study the chilled water system on a cruise ship and find ways to save energy. The focus is on optimizing the pumping methods in the system and to validate these savings. The thesis should also include a theoretical research part on

maritime and land-based air-conditioning basics as well as different pumping methods already in use.

The optimization of the different pumping methods is realized by building a dynamic simulation model. The model should be used to validate potential savings of different pumping methods, building it so that it can be further developed and integrated in a larger simulation model of the ship.

2. Background

Shipyards are under growing pressure to reduce ship pollution and increase energy efficiency. International organizations, national legislation and customers all demand higher energy efficiency to reduce global warming. International organizations, including the European Union and the International Maritime Organization (IMO), monitor emissions and introduce new regulations.

The IMO was initially introduced in 1948 as part of the United Nations to promote maritime safety. In 1973, measures were introduced to prevent pollution from ships. Today, IMO's environmental vision is to "eliminate, or reduce to the barest minimum, all adverse environmental impacts from ships" (IMO, 2011). To achieve the vision several regulations have been introduced. Many include minimizing airborne emissions, such as sulfur oxides and nitrous oxides, while others are more general, often energy efficiency-related ones (IMO, 2018a).

The IMO has three initiatives for greenhouse gas emissions control; the Energy Efficiency Design Index (EEDI) and Ship Energy Efficiency Management Plan (SEEMP) are mandatory initiatives while the Energy Efficiency Operational Indicator (EEOI) is voluntary. EEDI is used in the design and construction phase to calculate and measure the performance of the ship hardware. EEOI is a similar indicator for measuring the operation of the ship after construction. SEEMP is a mandatory manual used in the operational phase to improve energy efficiency through changes in operation (Abouelkawam, 2017).

The EU requires all large ships to monitor their annual emissions and other relatable information if they are using EU ports. The EU works in close collaboration with the IMO to have a global approach to reducing emissions. In addition to monitoring the emissions, the EU also has a strategy and is a large funder of IMO projects. The EU strategy involves monitoring of emissions, setting a reduced emissions target and further market-based long-term measures (European Commission, 2018).

Customers also demand better energy efficiency without compromising passenger comfort or experience. To the ship owner, improved energy efficiency means direct savings in operational cost, but it is still important that the energy efficiency investments have a short enough pay-back time to make them a financially viable option.

2.1. Energy Efficiency Design Index

The EEDI is one of the most relevant technical measures in terms of emission regulatory for the shipyard as it is mandatory for all new-built cruise ships using non-conventional propulsion, including, e.g., diesel-electric systems. This drives the yard to improve the ships' energy efficiency to meet stricter guidelines. There is today a need for more cruise ships as the number of cruise passengers is increasing strongly, by 20.5 % in the years 2011 to 2016 (CLIA, 2018). All new ships need to follow these requirements.

The EEDI is used to make a fair comparison of the energy efficiency of a new ship with a minimum required efficiency value. The EEDI represents energy efficiency as CO₂ emissions per travelled tonnage nautical mile [g CO₂/tn m]. The minimum required EEDI is tightened every five years until 2025, when a 30 % reduction is required compared to an average based on ships built between 2000 and 2010. The requirements after 2025 are not yet decided (IMO, 2018b).

The reference EEDI at 2010 for a cruise ship can be calculated based on the ship size in gross tonnage. The reference line value is calculated as $170.84 \cdot b^{-0.214}$, where b is the gross tonnage. The reference equation indicates that larger ships have a stricter reference point. Figure 1 presents the reference line for different gross tonnages (IMO, 2013b).

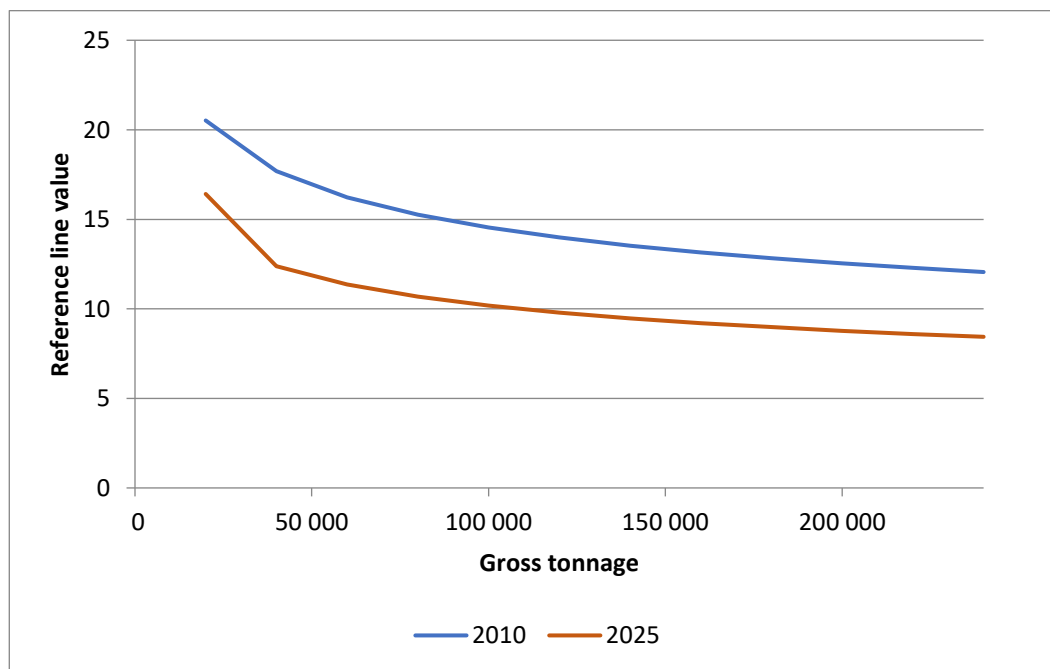


Figure 1: Reference EEDI for different cruise ship sizes, year 2010 and 2025

To calculate the EEDI for a new ship the following equation is applied

$$EEDI = \frac{\sum_{i=1}^{nE} C \cdot P \cdot SFC}{GT \cdot v_{ref}},$$

where nE is the number of engines, C is the carbon emission factor [g CO₂/g fuel], P is the engine power [kW], SFC is the specific fuel consumption [g/kWh], GT is the gross tonnage [GT] and v_{ref} is the reference speed of the ship [knots]. The engine power P is scaled from the installed power to obtain the actual used power (IMO, 2013a).

A final verified EEDI is determined at sea trials. The power curves from the sea trials should be compared with the calculated power curves from the design phase. A new EEDI should be calculated, if these power curves show differences. Likewise, possible differences in the final gross tonnage, ship speed or specific fuel consumption lead to recalculation of the EEDI (IMO, 2014).

The EEDI is very flexible, as there are no regulations on how the energy efficiency is reached. In collaboration with the customer the ship yard can find the most cost-efficient way to reach the reference point (IMO, 2018b).

2.2. Customers and passenger requirements

Customers, i.e. the ship owners, often set even stricter requirements on new-built ships than the international organizations. The ship owners usually have their own sustainability goals and programs to reduce emissions and environmental impact. These goals and programs usually specify energy efficiency separately.

Royal Caribbean Cruises Ltd. (RCCL) have their own environmental program "Save the waves" and strict requirements. They have collaboration with the WWF that sets goals that are to be reached by 2020. The most engaging of these goals is a reduction of greenhouse gases by 35 % compared to the 2005 level. RCCL have three ways to achieve these reductions: decreasing energy use, reducing emissions by better technologies and using alternative fuels and renewable energy sources (RCCL, 2017).

The world's largest cruise company, Carnival Corporation & plc (CCL), which owns 10 cruise line brands such as AIDA, Carnival, and Costa and over 100 cruise ships, also have similar environmental programs and goals (Carnival Corporation, 2018a). They have a goal of reducing carbon dioxide equivalent (CO₂e) emissions by 25 % by 2020 compared to the 2005 level, which is not quite as much as RCCL. They also have other goals, such as waste reduction, waste water purification and exhaust gas cleaning, and are also

increasing Cold Ironing coverage, which is the ability to connect to shore-side electrical power at port and turning off the ship engines (Carnival Corporation, 2018b).

Ship owners benefit considerably from increased energy efficiency, which makes it very important. Fuel costs are a big part of the cruise operating costs, and increased energy efficiency implies direct savings in costs. Figure 2 shows fuel costs compared to total operating costs and total cruise operating costs for RCCL. In the last three years, the fuel costs have been on average 15 % of the total cruise operating costs and 10 % of the total operating costs (RCCL, 2018).

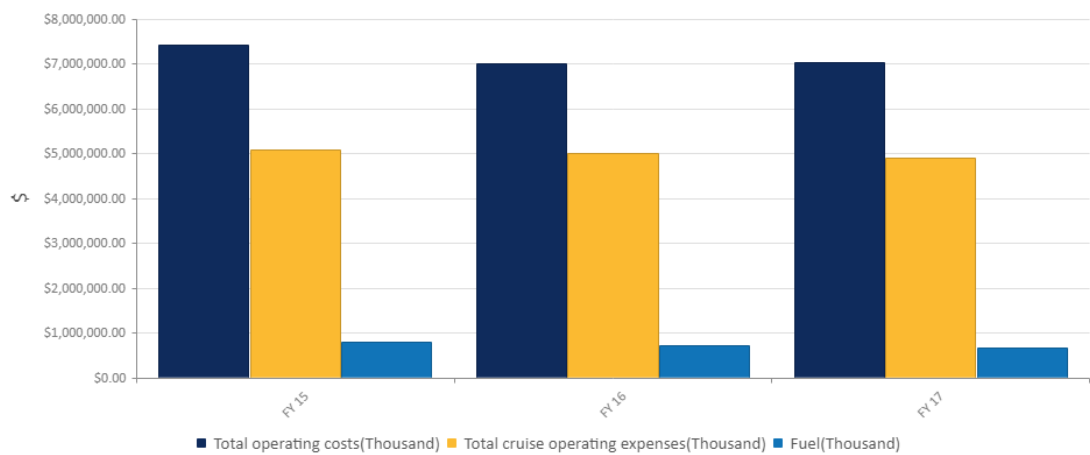


Figure 2: RCCL fuel costs during the years 2015-2017 (RCCL, 2018)

Some passengers are all the more environmentally knowledgeable and often take the environment into consideration when making a decision on their trip. Many cruise lines know this and use energy efficiency investments in their marketing. For example, Viking Line uses the fact that they have the newest and most energy efficient cruise ferry on route between Turku (Finland) and Stockholm (Sweden) in their marketing (Viking Line, 2018).

Even though passengers want environmentally sustainable cruises, they don't usually want to sacrifice experience. Therefore, the shipyard and ship owner need to find a way to increase energy efficiency so that it does not affect the passenger experience negatively. This can, for example, be by using more advanced technology, such as better pumping methods in the chilled water system or better operational strategy. Other examples how to improve energy efficiency without sacrificing customer experience is to apply a more hydrodynamic hull design, better waste heat recovery and more efficient electric power generation.

2.3. Literature review

Some studies have been undertaken on different pumping methods for chilled water systems. Earlier studies mainly concerned land-based office buildings or campuses, but their findings are still relevant for marine applications. The savings potential from different methods is mainly due to lower pumping costs but there is also a potential for more efficient chillers (Lee & Cheng, 2012). The consumption pattern and climate are important factors for the potential savings, which makes it hard to compare earlier studies with the cases in this thesis.

Figure 3 shows the pumping power dependence on ambient temperature for a single circuit with constant flow-pumping, a dual circuit with constant flow primary-pumping and variable speed secondary-pumping and a single circuit with variable speed-pumping. The pumping method cannot decrease the pumping power much if the heat load is high, but it is quite uncommon that the heat load is high all the time; the load usually depends on the time of day and season of the year (Tirmizi, Gandhidasan, & Zubair, 2012).

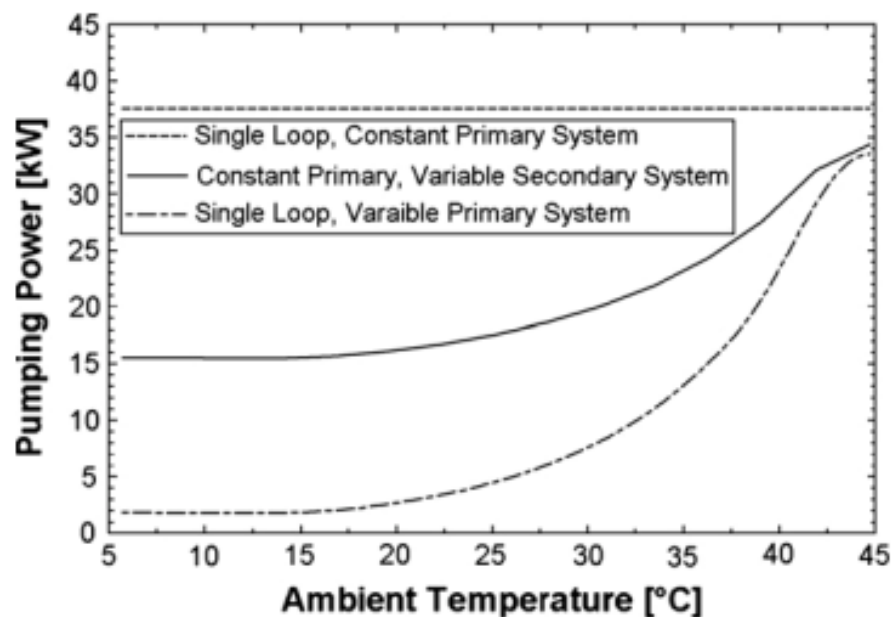


Figure 3: Pumping power dependency on ambient temperature (Tirmizi et al., 2012)

Kirsner (1996) criticized the primary-secondary design already more than 20 years ago. The primary-secondary design is a major cause of “low ΔT syndrome”, where the returning chilled water temperature is too low, causing a low temperature difference over the chillers. Furthermore, new chillers with more advanced controller units do not

require a constant flow to function properly, as they can handle large flow differences. There could be some use of a secondary pumping circuit in a large system, such as a campus, but this would not be applicable to cruise ships.

Yu and Chan (2008) pointed out the complexity of a variable primary flow, especially concerning bypass control for low loads and good staging of the chillers. These issues can be solved through good system design and modern control logic. They also highlighted that there is limited documentation on how much the variable chilled water flow through the evaporator affects chiller COP. According to their study, the COP can rise by 2 % when variable speed drive (VSD) chilled water pumps with an air-cooled centrifugal chiller are implemented. Furthermore, the power consumption of the pumps is reduced by another 2 %.

Bahnfleth and Preyer (2001) also found some significant savings by changing the pumping scheme. With a single chiller plant the pumping power saving with a variable flow primary pumping was 80 % compared to the constant flow primary method. Similarly, a primary-secondary setup yielded 59 % saving. The saving potential between variable primary flow and primary–secondary flow was smaller with more chillers. There is still a capital cost saving with primary only over a primary-secondary setup.

These studies all indicate savings with improved pumping methods, both in pumping power and chiller efficiency. The reduction in pumping power seems to vary considerably depending on consumption patterns and system setup. Even though these studies were all made on land-based CWS, the findings are applicable to cruise ships since the systems are quite similar. Cruise ships often have different itineraries depending on season and passenger need. Different itinerary locations yield different cooling needs and the chilled water system must handle it in an energy-efficient way.

2.4. Savings potential

Some calculations can be made to get an indication of the saving potential. By analyzing data from an existing ship, the average load and number of chillers can be calculated, as presented in Table 1. The existing ship and data are also used for validation in Chapter 7.

Table 1: Average CWS load for the validation ship

Average data	
Number of chillers running	2.1
Chiller load	76 %
Numbers of secondary pump running	1.3
Secondary pump load	53 %

The ship under consideration has a constant primary – variable secondary pumping system. The pumping power is directly proportional to the volume flow rate. There should be some potential savings, as the primary pump is sufficient for running the chiller at full load, and it is therefore pumping at an unnecessarily high speed.

The following three cases are studied for estimating the potential savings:

1. Constant flow
2. Constant primary – Variable secondary
3. Variable flow

All the pumps run at full speed in Case 1, which is the baseline case and it is presented in Table 2, and denoted as 0 % savings. In Case 2, the primary pumps run at full speed with chiller-dedicated pumps and the secondary pumps run with a constant differential pressure. In Case 3, all pumps run with a constant differential pressure.

Table 2: Potential savings in pumping power in the different cases

Case	Potential savings in pumping power	Potential saving in CWS
Constant flow	0 %	0
Constant primary – Variable secondary	71 %	10 %
Variable flow	74 %	10.5 %

Table 2 indicates large savings in the CWS pumping power for both Case 2 and Case 3 compared to the baseline case. The pumping power represents less than 20 % of the total energy consumption in the system, but the savings are still substantial for the CWS. Comparing Case 2 with Case 3 shows potential savings of 11 % in pumping power.

3. Air conditioning theory

This chapter will deal with the basics of air conditioning. Air conditioning is the process of cooling and dehumidifying the air to a comfortable level. The focus will be on big systems that are applicable on cruise ships. Large luxury cruise ships in the Caribbean and Mediterranean regions often have cooling powers in the order of tens of megawatts. For example, a cruise ship with a gross tonnage of around 200 000 would have a maximum dimensional cooling power load of approximately 30 MW in extreme conditions. Cruise ships that are planned for Mediterranean and Caribbean cruises are often dimensioned with a water temperature of 32 °C and, furthermore, need to have some chiller redundancy.

Air conditioning in luxury cruise ships is often the second largest energy consumer on board (Cao, Lee, Hwang, Radermacher, & Chun, 2015). The outside temperature can be up to 34 °C with very intense sun. The cooling need varies a lot depending on sun intensity and outside temperature.

The cooling can be achieved with many different methods. The traditional method is a heat pump using sea water as heat sink. The heat pump efficiency is very high with a COP value of over 5, but the power consumption is still very high.

There are a few waste energy sources onboard that can be used for free or cheaper cooling. Many new ships use liquefied natural gas (LNG) as an energy source. LNG is stored at a temperature of -160 °C and is heated to 30 °C before the engines. This is a free source of cooling that can be used. Absorption is another way to use waste engine heat for cheap cooling.

3.1. Air properties

The right air humidity and temperature are very important properties to a good air quality. The air will be perceived as less acceptable with higher temperature and higher relative humidity. There will also be a significant risk of condensation in the channels if the relative humidity is close to a 100 %. Condensation can result in mold, corrosion and other types of deteriorations (Fang, Clausen, & Fanger, 1998).

The relative humidity, φ , is the mole fraction of water vapor, x_w , in air to the saturated mole fraction of water vapor in air, x_{ws} (Wang, 2001)

$$\varphi = \frac{x_w}{x_{ws}}$$

The mole fractions, x_w and x_{ws} , are defined as

$$x_w = \frac{n_{water}}{n_{air} + n_{water}},$$

$$x_{ws} = \frac{n_{ws}}{n_{air} + n_{ws}},$$

where n_{air} is the moles of dry air, n_{water} is the moles of water vapor in humid air and n_{ws} is the moles of water vapor in saturated humid air. The relative humidity can also be expressed with application of the ideal gas law, $pV = nRT$, as

$$\varphi = \frac{p_w}{p_{ws}},$$

where p_w is the partial pressure of water in air and p_{ws} is the partial pressure of saturated steam in air. p_{ws} is a function of temperature and pressure since the relative humidity is dependent on the air temperature and pressure, because warm air can hold more water (Wang, 2001).

Air humidity can also be expressed as a humidity ratio which is the mass of water per mass of dry air (Westerlund, 2009)

$$\omega = \frac{m_{water}}{m_{dry\ air}}.$$

The easiest way to decrease air humidity in a cruise ship is to overchill the air by a few degrees and then re-heat the air to the set-point temperature. Air at 12 °C and 100 % relative humidity that is reheated to 14 °C has 88 % relative humidity, which is well below the dew point. The relative humidity is further dropped to 48 % at room temperature (24 °C).

The enthalpy of humid air can be calculated from the enthalpy of water and air

$$h = h_a + h_w,$$

where

$$h_a = c_{p,air}\theta,$$

$$h_w = h_{steam} + c_{p,steam}\theta.$$

The c_p values depend on temperature but can be approximated as $c_{p,air} = 1.008 \frac{\text{kJ}}{\text{kg}^\circ\text{C}}$ and $c_{p,steam} = 1.89 \frac{\text{kJ}}{\text{kg}^\circ\text{C}}$ in the ranges from -40 to 150 °C. The specific enthalpy of saturated steam at 0 °C is $h_{steam} = 2498 \text{ kJ/kg}$ (Westerlund, 2009).

The enthalpy in relation to different temperatures and humidity ratios is shown in Figure 4.

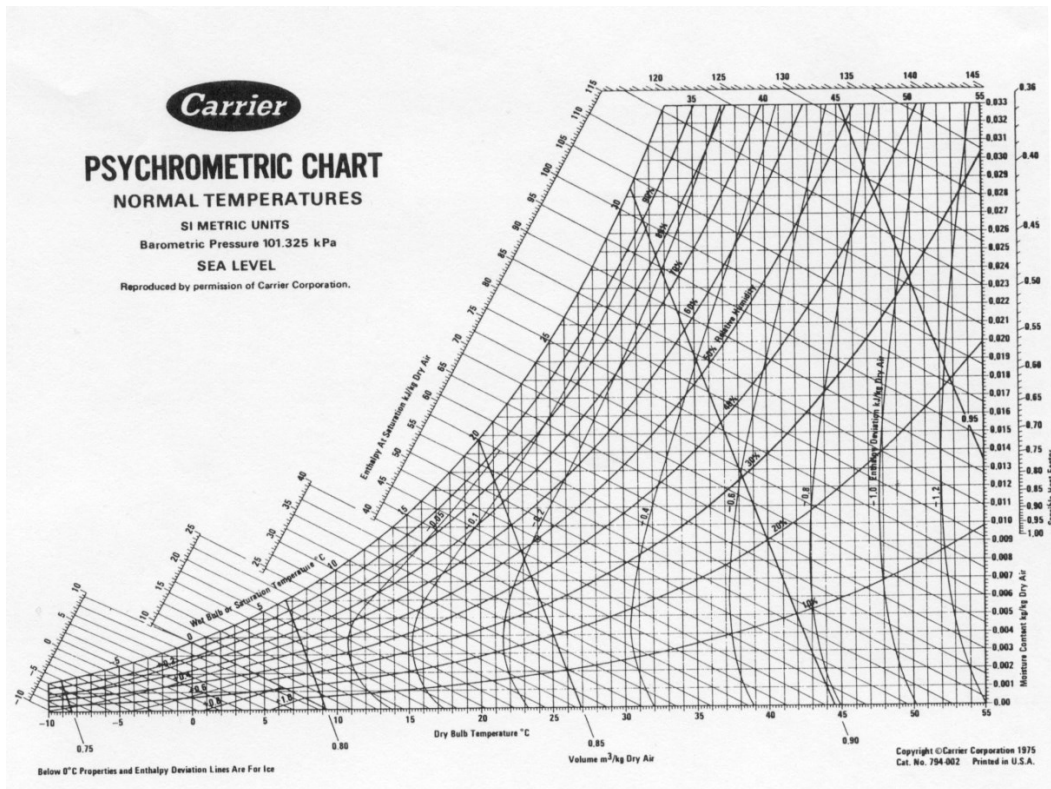


Figure 4: Psychrometric chart of humid air (Chegg Study)

3.2. AC chillers

There are various types of chillers used in marine applications. Electrical compressor chillers, LNG chillers, absorptions chillers and seawater coolers are treated in the following sections.

3.2.1. Electric compressor chillers

Electric compressor chillers are vapor-compressor refrigeration systems (VCRS) that produce chilled water for the HVAC system. They operate according to the same principle as in a refrigerator or household heat pump. VCRS are very energy efficient and can produce over five times more chilled water compared to the power input. The efficiency

is given by the Coefficient of Performance (COP), which is the ratio between energy output and energy input (Arora, 2012).

Figure 5 shows a typical continuous refrigeration cycle. Step 1 to 2 is the compressor that compresses the vapor refrigerant to a high-temperature and high-pressure state. Step 2-5 is the condenser that condenses the vapor into a liquid at the high pressure to a lower temperature. The condenser in a cruise ship is a seawater heat exchanger. The high-pressure liquid is next expanded in an expansion valve (Step 5-6) to a low pressure and low temperature liquid-vapor mixture. The low temperature liquid-vapor mixture is then evaporated into (superheated) vapor in Step 6-1. The evaporation step is used to cool the AC chilled water in a heat exchanger (Arora, 2012).

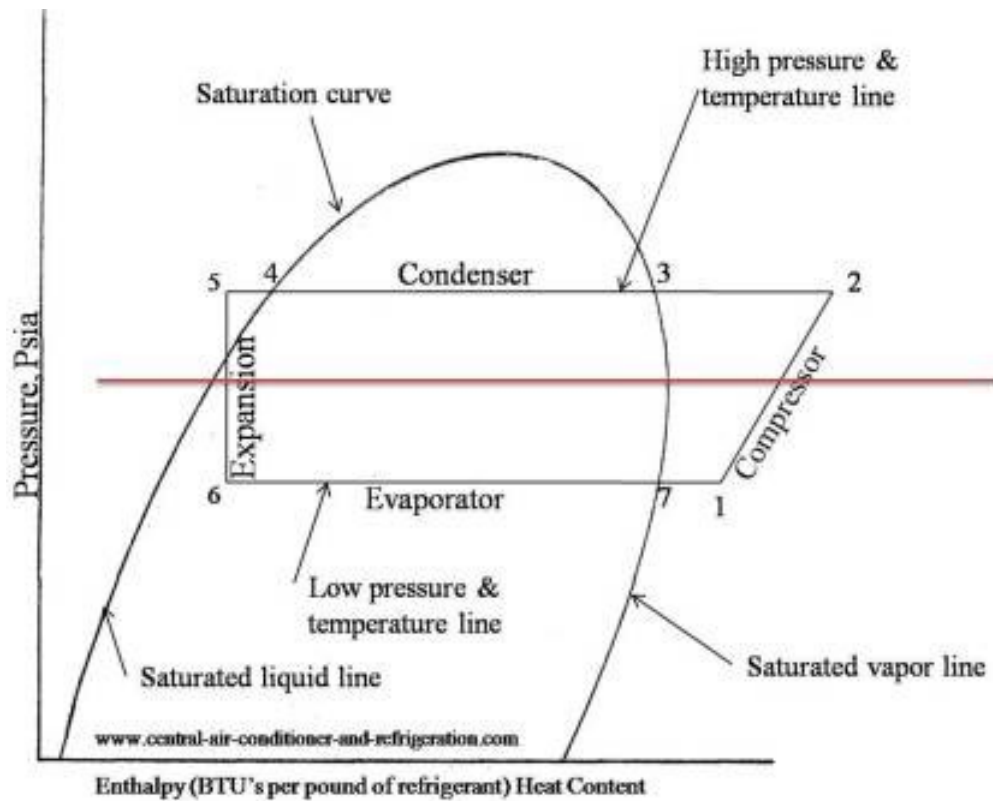


Figure 5: Electric compressor chiller working principle (Central-Air-Conditioner-and-Refrigeration.com)

The cooling power can be expressed as the product of the mass flow of the refrigerant and the difference in specific enthalpy over the evaporator, from Step 6 to Step 1

$$Q_c = \dot{m}_r(h_1 - h_6).$$

The power consumption in the chiller is that of the compressor and is illustrated in Figure 5 with Step 1 to Step 2. The compressor power needed to run the chiller is

$$P_{\text{comp}} = \dot{m}_r(h_2 - h_1).$$

A good refrigerant should have a boiling point below the desired chilled water temperature, with a high enthalpy of vaporization and a high critical temperature. The refrigerant should also have good environmental properties; it should not damage the ozone layer or cause climate change. The environmental properties are often given by the refrigerant ozone depletion potential (ODP) and global warming potential (GWP) which is a how much the gas contributes to global warming by a factor of carbon dioxide equivalents. Lower values on ODP and GWP are better as the environmental impact is lower. The ODP should be zero for all new refrigerants and GWP may vary between one, i.e. the same as carbon dioxide, and tens of thousands. It should also not be toxic for humans or corrosive in the refrigeration system. The most common refrigerant is R134a which has an ODP of 0 and GWP of 1430. New legislation could lead to a change from R134a to for example R1234yf, which has an ODP of 0 and a GWP of only 4 but is slightly flammable which is not desirable. (AGA industrigaser, 2018)

COP of electric compressor chillers

COP stands for coefficient of performance and is the ratio of useful cooling per input work or power (Arora, 2012)

$$COP = \frac{Q_c}{P_{\text{comp}}}.$$

The efficiency of marine AC chillers varies greatly with the sea temperature, as seawater is used for cooling in the condenser. This contribute to a decrease in cooling power at higher outside temperatures as well as an increase in cooling needs.

The theoretical maximum efficiency is called Carnot efficiency and can be calculated from temperature of the evaporator and condenser (Aittomäki, 2012).

$$COP_{\text{Carnot}} = \frac{T_{\text{cond}}}{T_{\text{cond}} - T_{\text{evap}}}.$$

The maximum theoretical COP calculated with an evaporator temperature of 6 °C and a seawater temperature of 18 °C and 30 °C is

$$COP_{18^{\circ}\text{C},\text{Carnot}} = \frac{291\text{K}}{291\text{K} - 279\text{K}} = 24.25.$$

$$COP_{30^{\circ}\text{C},\text{Carnot}} = \frac{303\text{K}}{303\text{K} - 279\text{K}} = 12.63.$$

The real COP can be calculated as the product of the Carnot COP and the system efficiency

$$COP_{\text{real}} = \eta_{\text{system}} COP_{\text{Carnot}}.$$

The system efficiency is usually around 50-70 %. The Carnot COP is almost twice as high at seawater temperatures of 18 °C compared to 30 °C.

3.2.2. Alternative chillers

Vapor-compressor refrigeration systems are very effective but still consume a lot of energy since the cooling needs are so big. There are some streams of free energy that can be utilized on large cruise ships. Many new ships are liquefied natural gas (LNG)-powered. The LNG has a considerable amount of cold energy available; LNG is stored at -160 °C and is used at 30 °C in the engines. Excess heat from the motors and exhaust gases can be used in an absorption chiller to generate chilled water. Alaska coolers are common in areas with colder sea water (Lepistö et al., 2016).

LNG chillers

LNG is natural gas in liquid form. At normal pressure natural gas is liquefied at -162 °C. LNG occupies only 1/600th of the volume of natural gas at the same pressure (Swedegas, 2018).

LNG can be held at slightly higher temperature if the pressure is higher, as seen in Figure 6. At 5 bar the storage temperature is -138 °C (Lepistö et al., 2015). The temperature of the natural gas fed to the engines should be 30 °C. The theoretical enthalpy change from LNG to gas can be found from the pressure-enthalpy diagram of methane. The theoretical available specific cooling energy is 900 kJ/kg but after losses in the system it is about 770 kg/kJ (Ukkonen, 2018).

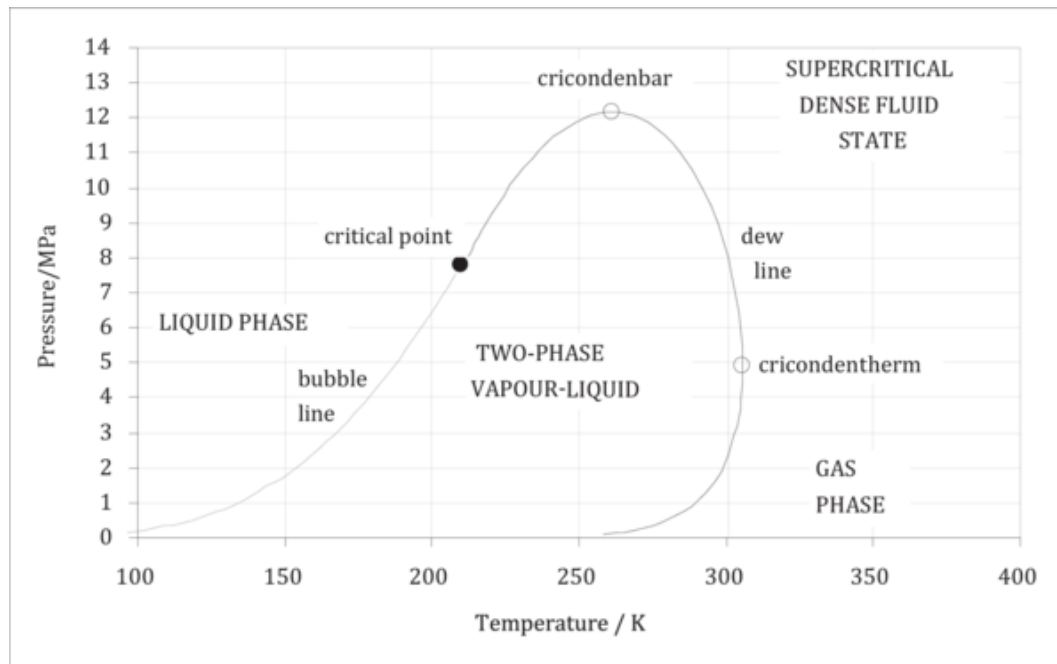


Figure 6: LNG phase diagram (ISO, 2015)

The cooling power of an LNG chiller can be calculated from the mass flow of LNG and the available cold energy

$$Q_c = \dot{m}_{LNG} \Delta h_{LNG} = \dot{m}_{LNG} \cdot 770 \text{ kJ/kg.}$$

The temperature difference between the LNG and the chilled water is big. The risk of freezing in the heat exchanger is large as the LNG temperature is well below the freezing temperature of water. Freezing can be avoided if the water circulation is fast enough or an additional circuit with a refrigerant is used (Ukkonen, 2018).

Absorption chillers

Absorption chillers work like vapor-compression refrigeration. The cooling is in both systems from vaporizing the refrigerant in the evaporator. The difference is that absorption chillers use a physicochemical process instead of a mechanical process, where the mechanical compressor has been replaced with a heat source. The basic principle is shown in Figure 7 (Horuz, 1998).

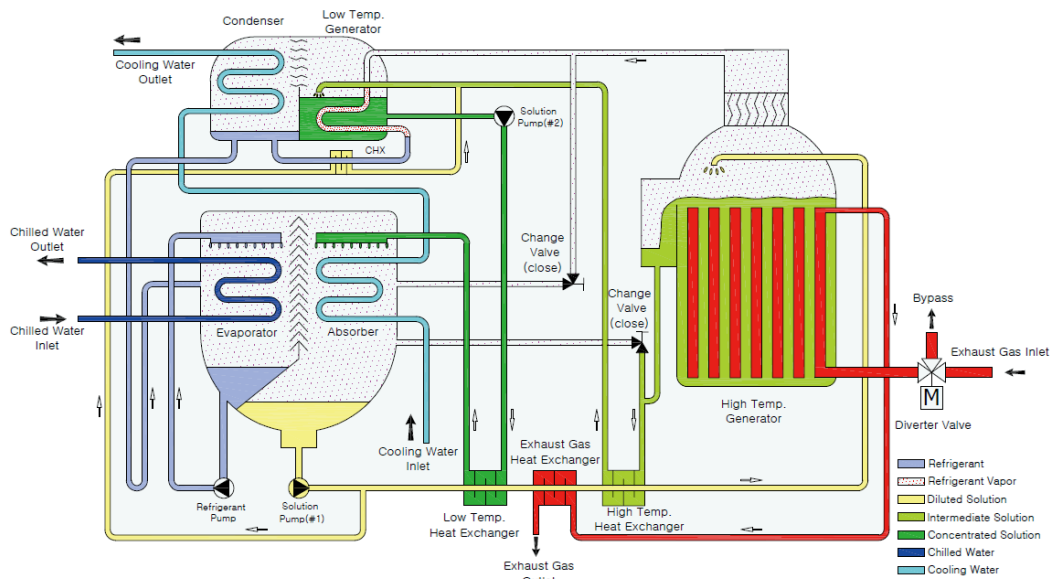


Figure 7: Absorption chiller principles (Goldman Energy)

Absorption chillers have a very poor COP compared to vapor-compressor refrigeration systems, but may still be beneficial if there is a cheap (or free) heat source available. The COP of absorption chillers is often in the range of 0.65-0.8 (Thermax, 2018). Large cruise ships often have substantial quantities of waste heat, especially at sea. This makes absorption chillers an interesting option for cruise ships.

There are some implementations of absorption chillers at large ships. One example is Eckerö Line Finlandia that has installed a 500 kW absorption chiller made by the company Gadlab. The installation on the Finlandia cruise ship has proven to work well and saves fuel and CO₂ emissions (Motorship, 2018).

Seawater coolers

Seawater coolers use sea water to directly cool the chilled water system with a heat exchanger. Seawater coolers only work if the sea water is cold enough, 10 °C or lower. The use is limited as the cooling need is quite low in areas where seawater coolers are usable (Lepistö et al., 2016).

The seawater flow needed is quite big as the temperature difference between the seawater and chilled water is low. The maximum cooling power of the seawater chiller is calculated from the water enthalpy and seawater mass flow

$$Q_C = \dot{m}_{sw}(T_{CWS} - T_{sw})c_{p,H_2O},$$

where \dot{m}_{sw} is the mass flow of seawater, c_{p,H_2O} is the specific heat capacity of water ($4.2 \frac{\text{kJ}}{\text{kgK}}$), T_{CWS} is the chilled water temperature and T_{sw} is the seawater temperature.

The actual cooling power is lower as it is dependent on heat exchanger area.

The seawater coolers provide very cheap cooling, since the only power use is in the pump. The pump can be controlled with variable speed drive to adjust the pump speed and save energy.

3.3. Reheaters

The reheaters have two different uses in a HVAC system. The main use is to work with the cooling coil to dehumidify the air. The supply air is cooled lower to remove enough moisture from the supply air. The reheater then heats the supply air to a suitable temperature. The reheat set-point temperature can be different for different spaces: for examples cabins should be reheated less on the sunny side of the cruise ship. The supply air is thus also above its dew-point, which prevents condensation of moisture. The reheater is also used during colder seasons to heat the supply air to a suitable temperature.

Reheaters can be either electric or warm-water circuits. Both are used in cruise ships for different applications. Electric re-heaters are cheaper to install, but are more expensive to operate. Warm-water systems can utilize waste heat and are therefore cheaper to run (Madison gas and electric, 2015).

The reheat energy need is much higher in colder seasons when the re-heater is partly used for heating the ship. This can easily be adjusted for with a warm-water system as the supply water temperature can be increased. In electric systems the re-heating coils have to be designed for winter conditions.

3.4. Air handling units

Air handling units (AHU) are a vital part of the HVAC system. AHU can, depending on application, have the following functions: intake of fresh air, outtake of used air, heat/cold recovery, cooling of the air, heating of the air, dehumidification and humidification. A typical cruise ship in the 100 000 GT size class has approximately 50 AHUs, where one AHU can serve 90 cabins with a combined size of 1400 m² (Nurmi, 2017). An example of an AHU is shown in Figure 8.



Figure 8: Air handling unit with enthalpy recovery wheel (Saiver)

The intake of fresh air and outtake of used air fluctuate based on air quality. Temperature, enthalpy, air humidity and carbon monoxide sensors are used to determine the air exchange needed. The air flow is controlled either by fan speed adjustments or dampers depending on the type of AHU. All AHUs do not have all the mentioned sensors or speed controlled fans (Meyer, 2018).

Heat and cold recovery can be used both in hot and cold climates to increase energy efficiency. Enthalpy recovery wheels (ERW) are used in most AHU on cruise ships, but some areas are exempt for hygiene or practical reasons. The ERW are used in three different modes, heating, cooling and stop mode, which are controlled based on outside air temperature and enthalpy. The ERW are used for heating when the outside air temperature drops below the supply air temperature, and for cooling when the outside

enthalpy (that is temperature and humidity) is above a set-point value. The speed is changed based on AHU supply temperature in heating mode and constant in cooling mode. The wheel is stopped if neither condition is met (Meyer, 2018).

The air passing through the AHU is heated, in addition to by the ERW, by the preheater and reheater. The preheater heats the air to a suitable temperature set by a PID controller; it will only heat if the ERW doesn't reach the temperature alone. The PID controller uses the supply air temperature and the set-point air temperature to drive the valve for the hot water heat exchanger. There is also a freeze alarm that opens the valve fully (100 %) at the preheater (Meyer, 2018).

The cooler is a chilled-water heat exchanger that is controlled by a PID controller to achieve a set-point temperature and humidity. The cooler is only used if the ERW does not reach the set point alone. The cooler and preheater are interconnected so that only one can be used at a time, not to waste energy by both heating and chilling. The cooler and preheater can also use the same coil to save costs, as only one is used at a time. The fan coil units handle all the cooling in that case. The air is also dehumidified with the cooler (Meyer, 2018).

There is also a need for humidification in cooler climates and seasons. The humidifier is controlled by the outdoor air humidity as well as the set-point humidity. The supply air relative humidity has to be less than 90 % to avoid condensation in the ductwork (Meyer, 2018).

3.5. Fan Coil Units

Fan coil units (FCU) are installed to help the AHU to control the temperature in the ship and provide additional cooling and heater power to certain areas. The fan coil unit is provided with air from the AHU that is mixed with recirculated air from the area. The fan coil units consist of a fan, a damper to control the mixture of fresh air and recirculated air, a cooling coil and in some cases a reheating coil. A typical FCU is presented in Figure 9 (Meyer, 2018).

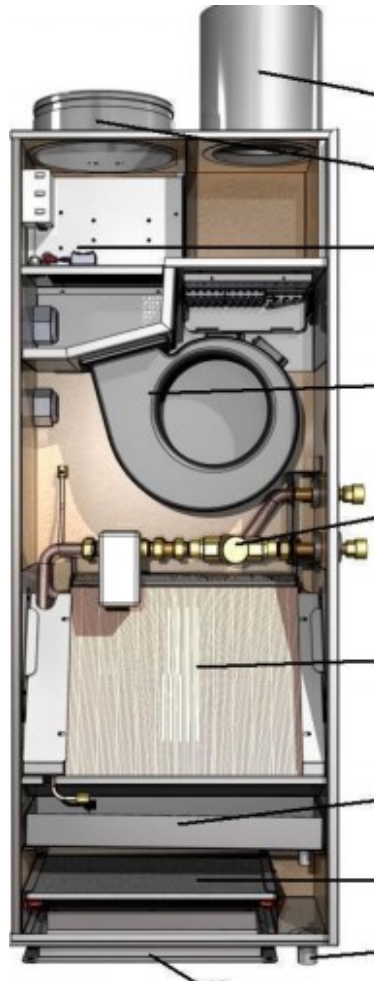


Figure 9: Fan coil unit (Hakala, 2012)

The FCU in public areas are always a cooler and reheater unit that compensates the variable heating and cooling needs. The cooling and reheater coils are controlled on the basis of inside and outside temperature sensors (Meyer, 2018).

Similarly, there are technical fan coil units (TFCU) in technical spaces, such as server rooms, to provide additional cooling. These do not have a reheater and are only used for cooling. The smaller TFCU are controlled locally by an output thermostat and the larger

sized TFCU are controlled by the ships automation system (constant set-point temperature) (Meyer, 2018).

The cabins also have fan coil units that are controlled by an adjustable temperature set-point in the cabin. The CFCU works as the public fan coil unit with both a cooler and reheater (Meyer, 2018).

4. Pumping methods

The most common pumping methods are constant flow, primary-secondary flow systems with constant flow primary and variable flow secondary (constant pressure difference) and variable primary flow (constant pressure difference).

4.1. Pump theory

Pumps work mainly by rotodynamic principles, for example by a rotating impeller, or by positive displacement principles, for example by displacing a trapped volume through the pipe. In theory, rotodynamic pumps have a constant relation between flow and pressure, and positive displacement pumps always have a constant flow. In practice, the pressure and flow are affected by changing efficiency due to limitations in the design, fluid properties or other contributing factors (Nesbitt, 2006).

The pumps used in CWS are always rotodynamic pumps, as they should handle variable flow and pressure. The most commonly used pumps are centrifugal pumps. Centrifugal pumps can efficiently pump large amounts of water at relatively high pressure, which is needed in the CWS.

The useful pumping output is defined as

$$P_u = \dot{m}g\Delta H = \rho\dot{V}g\Delta H,$$

where ρ is the density of the fluid, \dot{V} is the volume flow, g is the gravitational acceleration and ΔH is the differential head needed.

The actual pump power is determined by the efficiency of the pump:

$$\eta = \frac{P_u}{P}.$$

The peak pumping efficiency is usually in the range of 70-85 % with an additional loss at the electrical motor. The efficiency of an electrical motor is around 95 % (Meyer, 2018).

The efficiency equation can be combined with the pumping output equation and further simplified to give

$$P = \frac{\rho\dot{V}g\Delta H}{\eta} = \frac{\dot{V}\Delta p}{\eta}.$$

The combined equation shows that the pumping power is directly proportional to the volume flow and the pressure increase. To lower the pumping power either the flow or the pressure, or both, should be lowered.

The pressure is the internal pressure of the chilled water system. The height difference does not contribute here, as it is a closed system. The pressure loss arises from a combination of piping, valves, bends, heat exchangers and other system components (Nesbitt, 2006).

4.2. Constant flow

The constant flow pumping scheme, shown in Figure 10, is the oldest and most simple pumping scheme. There is no control involved and the water is always pumped at full speed through the whole system. This is very inefficient, as all the pumps are always running at full speed and the worst case scenario is that the air is cooled more than needed and needs to be reheated. The efficiency can be improved somewhat with a 3-way valve for bypass at the AHU (air handling unit) that is controlled by the outgoing air temperature.

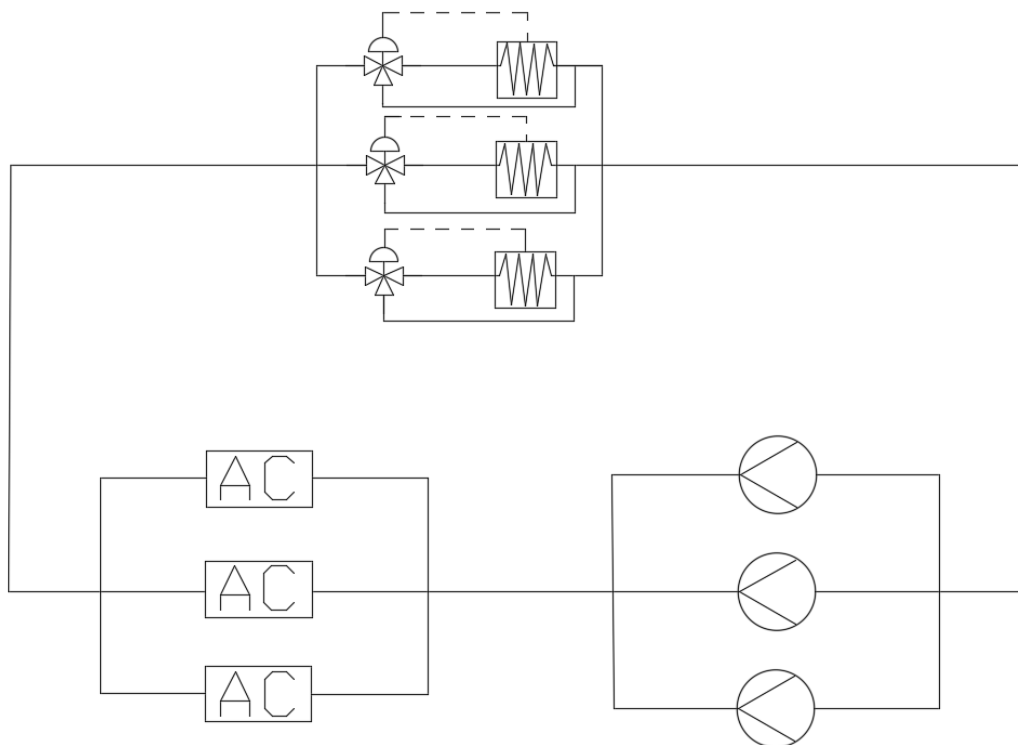


Figure 10: Constant flow pumping method

Usually, the chillers are controlled so that the return water temperature is 13 °C. This leads to a very low temperature difference over the chillers at lower loads, which is not ideal as the logarithmic mean temperature difference is reduced leading to a reduced heat transfer.

The investment cost is low for the constant flow concept, as there is no need for frequency controllers, extra pumps or additional bypass piping.

4.3. Primary–secondary flow

A constant primary with a variable secondary, shown in Figure 11, has been the most common land-based scheme for decades (ASHRAE, 1996). The primary loop has no control and is always pumped at full speed. The secondary loop is equipped with a controlled variable speed pump. The water feed to the AHU is controlled by a 2-way valve that is set by the outgoing air temperature.

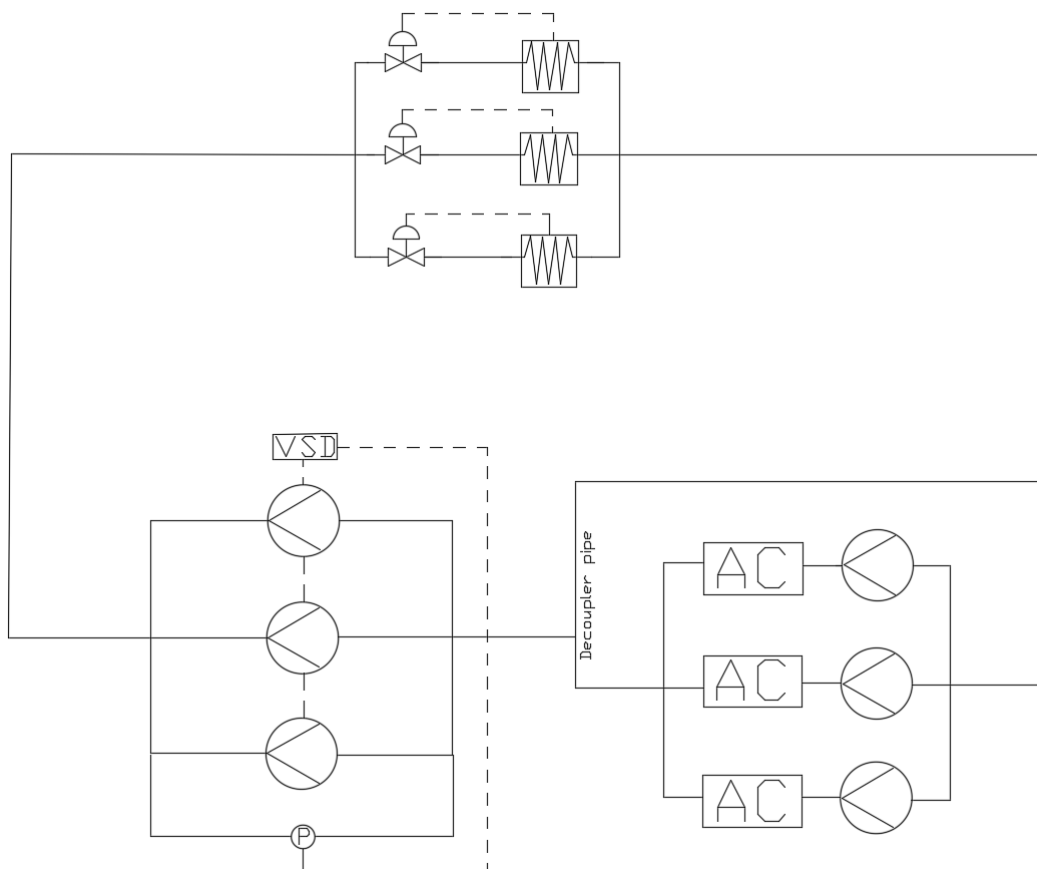


Figure 11: Constant primary - Variable secondary pumping method

Primary-secondary flow does not solve the problem with low temperature difference over the chillers. It does, however, give a better temperature control at the AHU and has

a saving potential at low loads, as the water does not have to be pumped all the way to the AHU.

There is also a need to control the secondary flow so that it is not greater than the primary flow. This can be done with a check-valve at the decoupler piping.

The investment cost is higher, as there has to be a pump in the secondary circuit as well. The frequency control can also be quite expensive. Furthermore, there are also some extra piping costs for the primary circuit bypass (Tirmizi et al., 2012).

4.4. Variable flow

Variable flow systems, shown in Figure 12, have always been technically feasible but the control system has been considered too complex. Recent developments of control systems have made it feasible today.

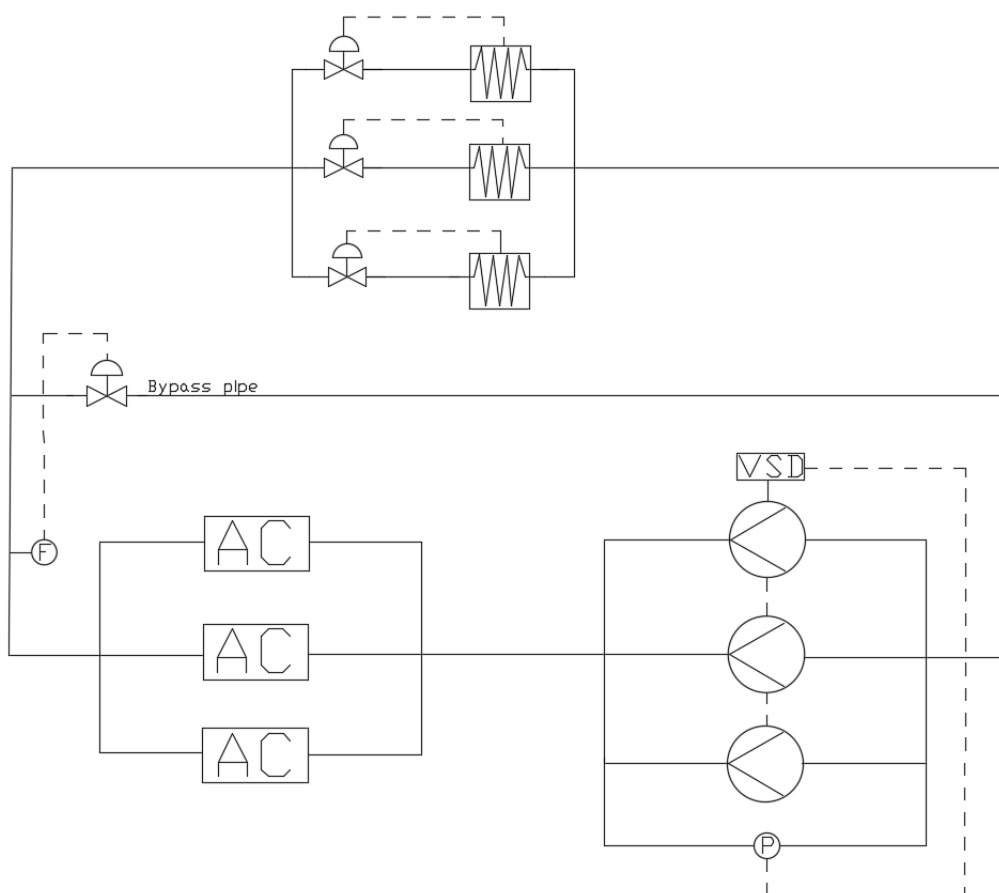


Figure 12: Variable flow method

There are a few vital points that make the control more complex. The AC chillers often need a minimum flow through them to prevent the evaporator from freezing and for

achieving proper cooling (turbulent flow). This can be achieved with a bypass that is only used if the flow rate drops too low. There can also be some difficulties if the flow rate changes quickly, for example when a second chiller/pump starts. It is also important to have a high enough pressure difference so that all the consumers receive enough water at high loads.

The system is somewhat similar to the primary-secondary system. The AHUs are controlled with two-way valves by outgoing air temperature. The pressure differential in the system controls the main pumps. There can also be a bypass that opens, if the flow rate drops too low.

The investment cost for variable flow systems is lower than for primary-secondary systems, as there is no need for the secondary pumps (Tirmizi et al., 2012). The control system is more expensive and requires more sensors. The total investment cost is around 5 % lower than for the primary-secondary system (Johnson Controls, 2017).

The running cost should also be lower, as the pumps can run at better efficiency and no excess water is pumped.

4.5. Dedicated or manifold pumps

The pumps can either be manifold or chiller-dedicated. These configurations have a difference in primary-secondary and variable flow systems.

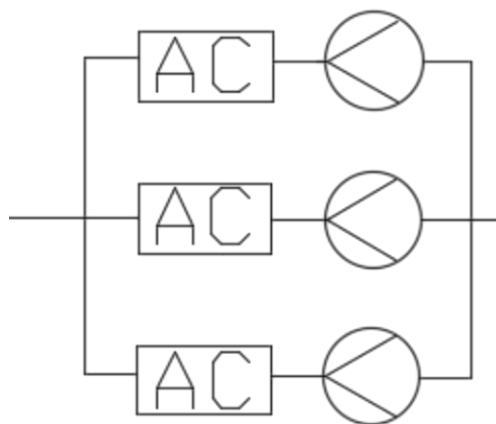


Figure 13: Dedicated pumps

A dedicated pump to each chiller, as seen in Figure 13, is easier to control as the chiller and pump are always running together. Dedicated pumps also simplify system hydraulics as the changes are small when a second chiller is started (Trane, 2011). Dedicated pumps

can also give some energy efficiency improvement if the chillers are of different sizes as the pumps can be differently rated according to pressure drop and flow (Taylor, 2002).

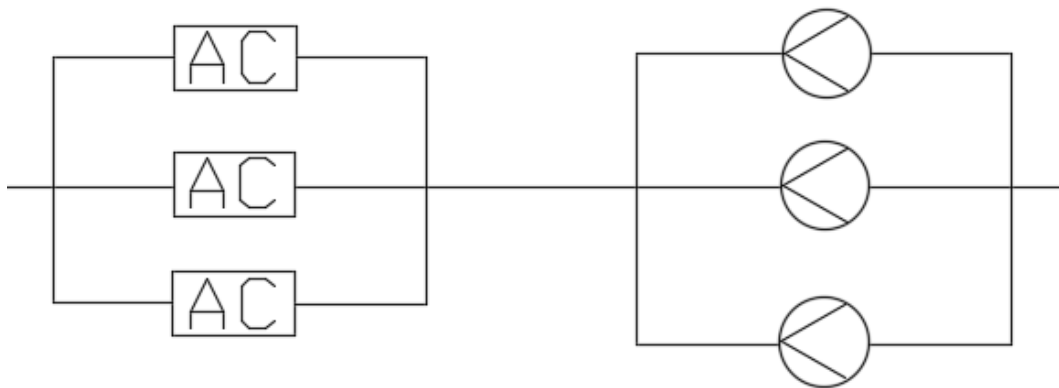


Figure 14: Manifold pumps

Manifold pumps, as seen in Figure 14, give some more redundancy as the chiller can be used even though the pump is not working. Redundancy can be improved easily with an extra stand-by pump that can serve any chiller (Taylor, 2002).

In the variable flow case, the manifold configuration is more energy efficient as the pumps can be run at optimal efficiency (Tirmizi et al., 2012).

5. Simulation tool

Dynamic simulation is the most suitable method to examine the pumping methods and to determine the energy saving potential for the system at hand since the reference ship has not been built yet and actual experiments would be very expensive and difficult to do. Dynamic simulation software describes the process with mathematical models such as differential equations and solves them numerically through a time interval with the current system model parameters.

The uses of dynamic simulation are many. It can be used to prove a concept, for system operation development, safety testing, operator training, system stability testing, automation parameter testing and energy efficiency testing (Barton, 1997).

The difference between dynamic and steady state simulations is the ability to predict dynamic changes. Dynamic simulation software is able to capture the key performance of the process system. This gives a tool that can simulate the operation similarly to the real system (Lappalainen, Blom, & Juslin, 2012).

There is a lot of different dynamic simulation software that have different applications. Some examples of dynamic simulation software are Aspen Plus, which is specialized for chemical industry processes, and MathWorks Simulink that is a more general tool (Aspen Tech, 2018; MathWorks, 2018).

5.1. Apros dynamic simulation tool

Apros 6 Combustion was chosen for the simulations. Apros is an advanced process simulation software developed by VTT and Fortum for thermal power plants, but it can be used for many different plants and processes as well. The software combines a graphical interface used to build the process and automation models with accurate thermal hydraulic solvers (Apros, 2018).

Apros has a built-in library with both process and automation components. The process library contains all vital components for a ship's chilled water systems, such as piping, pumps, heat and cooling sources and different types of valves. Figure 15 shows an example of a process diagram built in Apros (Apros, 2018).

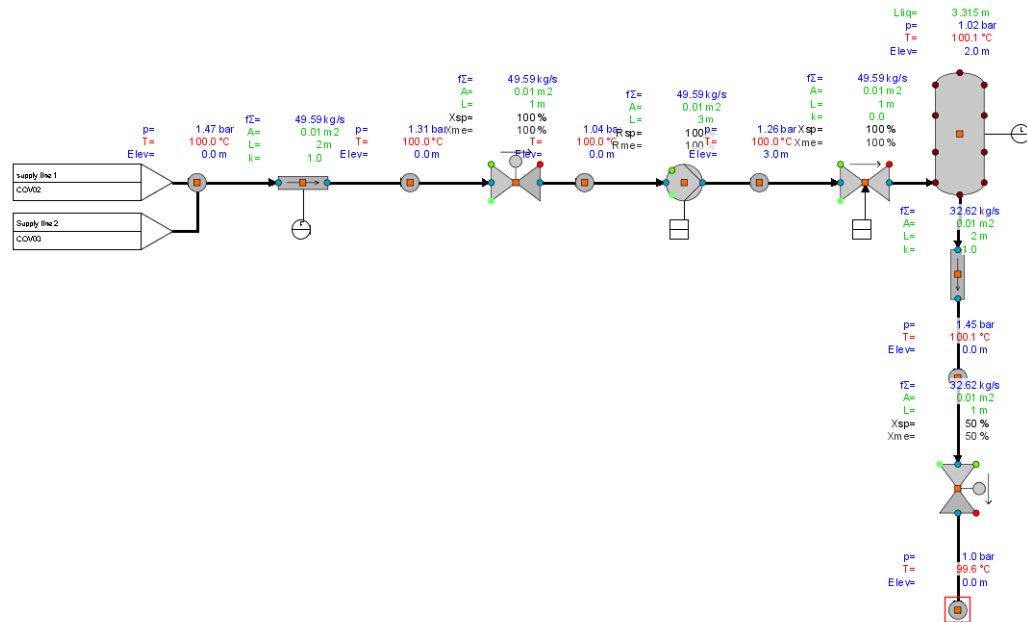


Figure 15: Example of Apros 6 process diagram

The automation library contains the automation components needed such as (e.g., temperature and pressure) sensors, controllers, actuators and basic analog and binary components (e.g., limits and set points). Figure 16 presents an example of an automation diagram in Apros (Apros, 2018).

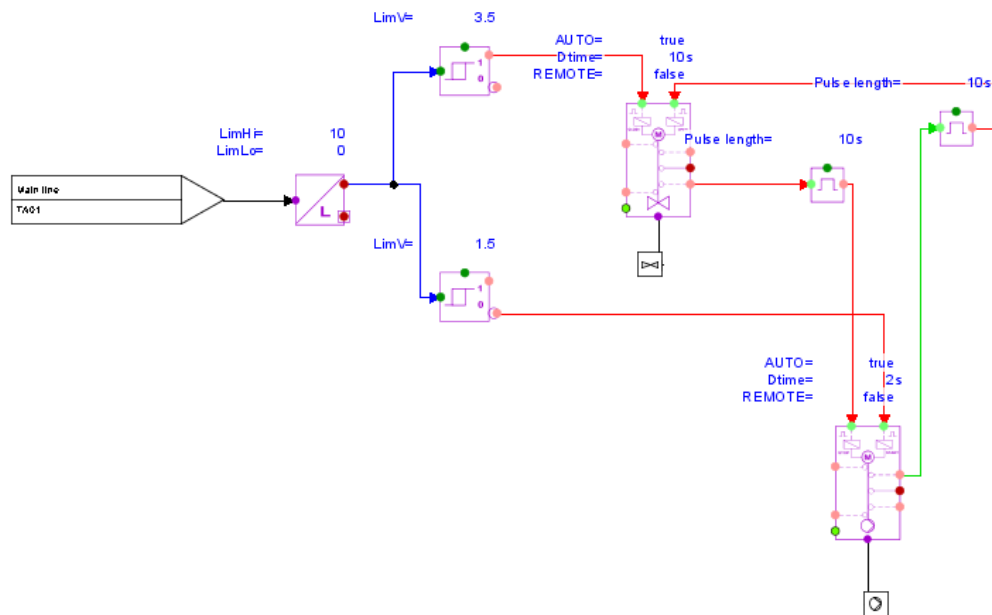


Figure 16: Example of Apros 6 automation diagram

Apros requires component data to obtain a good and accurate model. The different process components should be set up with data from the actual components. For example, pump set-ups include data for the pump curves and pump dimensions. The controllers are set up with the widely used PID parameters (Apros, 2018).

Apros has three different thermal hydraulic model solvers built in for different applications: a homogeneous 3-equation model solver, a drift flux 5-equation model solver and a two-fluid 6-equation model solver. For example, the model solvers are used to simulate mass flow, momentum, energy and mass fractions (Tuuri & Paljakka).

Apros has been thoroughly validated with over 70 different cases and is checked by several validation cases at every major version update (Ylijoki et al., 2015).

6. Model set up

The model is built in Apros 6 with the built-in graphical user interface. Apros process builder has a lot of process components included and the process model can be built easily by the drag-and-drop method. The automation builder has a similar system for the automation structure.

To get a good and representative model of the system, but to avoid excessive work in the set-up and too long computation time, some assumptions have to be made. It would not be suitable to include every chilled water consumer throughout the entire ship, as this would make the simulation model very slow as well as hard to manage. Additionally, it would be very difficult to acquire and manage the consumer data. A well-built model with reasonable simplifications concerning the consumers and piping will still represent the real-life situation.

A typical large cruise ship is divided in six to eight vertical main fire zones and usually has 16 to 19 decks. The height difference is substantial as the chillers are located at the bottom of the ships, over 50 meters at most. The internal pressure of the system needs to be high enough to overcome the height difference. However, the height difference does not increase the pumping power as it is a closed system. The reference ship has seven fire zones and 19 decks. Each fire zone has a main vertical chilled water pipe that is branched into smaller pipes at the different deck levels.

The significant pressure drops occur at a few main points. The largest pressure drop is at the chillers, as they require fast turbulent flow to achieve decent cooling. The chillers need a minimum evaporator water flow rate of 1.2 m/s (Johnson Controls, 2018). Other large pressure drops occur at valves, piping and cooling coils.

The actual piping dimensions and consumer data were used to build the model. The consumers were simplified to a maximum of one per deck and fire zone. The simplification can be justified as all the chilled water consumers are connected in parallel and all the cooling coils are dimensioned to have a similar pressure drop, assumed to be 50 kPa at full load at all consumers (Meyer, 2018).

The piping is dimensioned to have a slow laminar flow through the entire system to minimize the pressure drop. This is achieved by using big pipes near the chillers where the flow is high, reducing the pipe diameter as the flow is decreasing closer to the chilled water consumers.

The valves are also dimensioned to allow for a large enough flow to achieve sufficient cooling. The valves at the consumer units are automated so that the return temperature is constant, which is close to the conditions in the real automation.

Heat pipes are used to mimic the cooling coils in the AHU and FCU. This gives a similar effect as the cooling coil while being easier to control than a water-air heat exchanger. The heat pipe is controlled by heating power of the pipe wall in megawatts which can be easily controlled by a variable input data value.

Similar heat pipes are also used for the AC chillers. The cooling power is controlled by the negative heating power of the wall in MW. The automation is set up to control the output chilled water temperature by adjusting the cooling power and starting additional chillers if the cooling power is insufficient.

One of the more difficult tasks is to select suitable pumps for the different pumping methods. A ship is just planned for one of the methods and it can be a challenge to choose the other pumps in a realistic way. Different ships with different pumping methods were studied to find a suitable pump that could be scaled to achieve an appropriate result. Another challenge is the automation of the pumps and how they should operate, e.g., when the next pump should start. Since Apros has good tools for automation, a good automation model could still be worked out fairly easily.

The model is built with easy modularity to make it possible to switch between the different pumping methods.

The constant flow and variable primary flow methods are set up with manifold pumps before the chillers to give extra redundancy and possibilities for control. The primary-secondary pumping method is set up with chiller-specific primary pumps and secondary pumps at the inlet of the secondary circuit.

All the variable-speed pumps are set to work at constant pressure difference. The pressure is "measured" before and after the pumps and the difference is calculated in the automation system.

The variable primary arrangement is equipped with a small bypass pipe and a valve at deck 0 that is automated to keep the flow above the minimum flow rate. The primary-secondary arrangement is equipped with a large decoupler pipe next to the chiller.

6.1. Set point values

The model requires a lot of set points to achieve an appropriate result. Some of the set points are available from design documents while others had to be found. The automation systems can be set through testing and by making suitable assumptions.

The AC system in a cruise ship is controlled by the onboard automation system and the set points can be adjusted. Different ships often have different set points. In the present case, the set points are chosen to represent a typical cruise ship. The typical supply air temperature is 10 °C below room temperature, i.e. 12-14 °C. The returning chilled water temperature will be lower than the supply air temperature. In this case, the return chilled water temperature set point is set at 13 °C.

The outgoing temperature of the chiller should be low enough to keep the water flow low and high enough to keep chiller COP high. A chiller output of 6 °C is chosen in this case, which is a typical summer chilled water temperature. The set point could be higher under winter conditions.

The chillers are also set to have the same pressure drop as a real chiller. The pressure drop is set at the nominal flow. The pressure drop varies almost linearly from minimum to maximum flow (Meyer, 2018).

The valve speeds are chosen to represent a realistic actuator and to keep the process functional. The controllers' PID values are set by testing to achieve a fast and stable control.

The bypass valve is set to keep the chiller flow above the minimum. A flow meter is set-up after the chillers and the valve is controlled to keep the mass flow above 100 kg/s.

The pumps are set up by the head, NPSH and efficiency curves. These curves give a good model of the pumps and enable accurate simulation. The exponent head dependency can also be set for the variable speed pumps. The exponent dependency is here set to two.

The variable pump speed is controlled by a constant pressure difference. The difference is set to be big enough to supply enough water at the highest load to the consumer farthest away.

6.2. Automation control

The control is mainly needed in the chillers and consumers. The consumer control, seen in Figure 17, is based on a temperature sensor in the return chilled water. The controller

then adjusts the set point for either the three-way valve (constant flow method) or two-way valve (both variable flow methods) to achieve the desired temperature. The actuator drives the valve to the correct position.

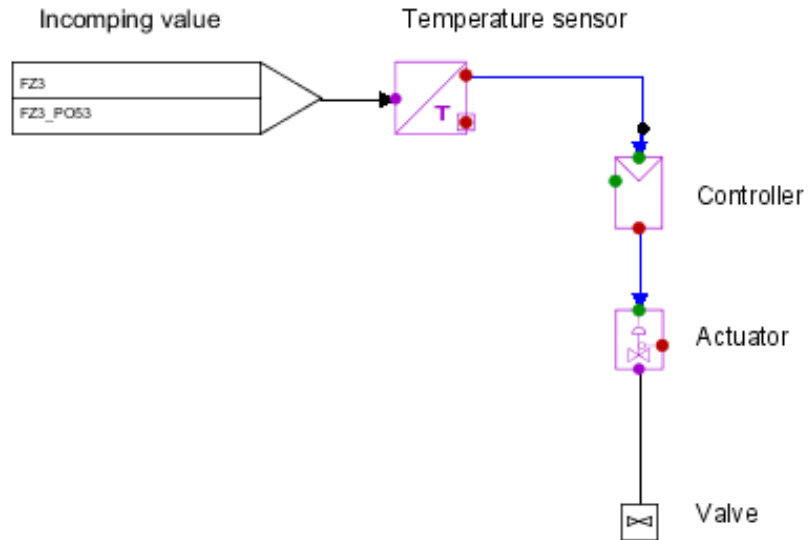


Figure 17: Automation of the consumer valve

The chiller control, seen in Figure 18, is based on the outgoing temperature of the chiller. The controller adjusts the chiller cooling power to reach the desired outgoing temperature. The value transmitter feeds the value to the chiller. Additional chillers are started if the cooling power of the chiller reaches its maximum and the desired temperature is not reached.

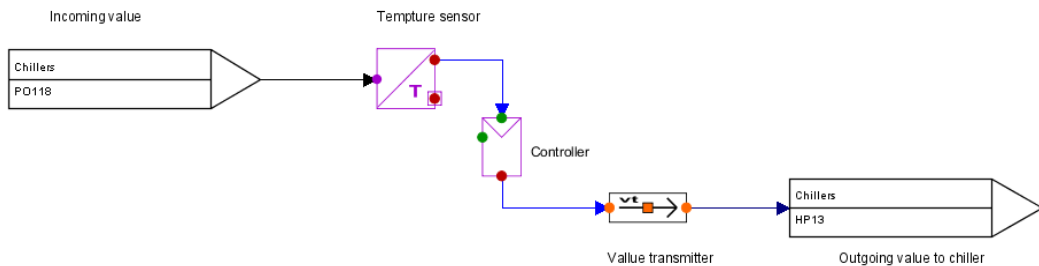


Figure 18: Automation of the chillers

6.3. Testing and optimizing the model

The model was built one fire zone at a time with simulation in-between to ensure a stable behavior. Maximum load was used in the building stage to ensure that enough water circulated. The chillers were adjusted to actual capacity in the end of the phase.

Some check-valves were added to ensure that the flow was in the right direction at all times, which is mainly important for the build- and set-up stage: the Apros simulations will crash if there are large flows going in the wrong way.

When all the fire zones were built and found stable at maximum load, variations of the load were simulated. To simulate a strong load variation, a sine-wave load was set at the consumers, with the difference of minimum and maximum load set as the amplitude over a period time of a couple of hours. It was found that the controller parameters had to be adjusted to manage the load changes efficiently, so they were re-tuned.

The internal pressure and pressure difference of the pumps were also set at maximum load to ensure a functioning system with enough capacity.

7. Validation

Validation is needed to confirm the accuracy of Apros 6 and the model. As the reference ship does not exist, data from an existing ship was used for validation. The available validation data is from a ship which is about 30 % smaller by gross tonnage than the reference ship and which has about 33 % less installed cooling power. The validation ship uses the primary-secondary pumping method, as it is the most common new pumping method. There was no data available to validate the other pumping methods. The validation procedure will compare Apros 6 output data with data from the actual ship.

The validation ship has the same numbers of fire zones and only one deck less than the reference ship, even though the validation ship is 30 % smaller. The piping network is quite similar which makes the adaption of the model easy. Some process modelling changes were still needed as the consumers appear on different decks.

The properties are quite scalable between the ships; most factors are close to the 70 % mark, as seen in Table 3. The installed cooling power is a bit higher on the reference ship as there is more alternative cooling methods that cannot be used at full capacity at all times. The additional alternative coolers do not affect the pumping system in a substantial way, as they can all be seen as a heat exchanger with different capacity.

Table 3: Comparison between reference and validation ship

	Validation ship/reference ship	
Gross tonnage	70 %	
Installed cooling power	67 %	
Length	79 %	
Width	77 %	
Passenger beds	86 %	79 %
Crew beds	63 %	

The validation ship is designed with two separate secondary flows, one for the fan coil units and one for air handling units. The secondary circuit for the air handling units is also used for heating in the winter and can in that case be separated from the primary circuit.

The supplied data had some limitation that had to be considered. The total supplied data sample was for a time period of four months, May to August, with a time interval of one

hour. The data was divided into fire zones by AHU type. The secondary pumps' power load and AC chiller load were available at intervals of 10 minutes.

Validation was only undertaken for the AHU secondary circuit since the available data was more comprehensive. The cooling loads were reported in electric consumption equivalents and had to be multiplied with the available COP value of the chillers to get the actual cooling load. To get a fair consumption distribution, the cooling load data was divided by fire zones and decks by analyzing the load data per type and the ship's deck plan. A time period of 71 days from June to August was selected as these days showed a suitable load variation. The total cooling load on the AHU units is depicted in Figure 19.

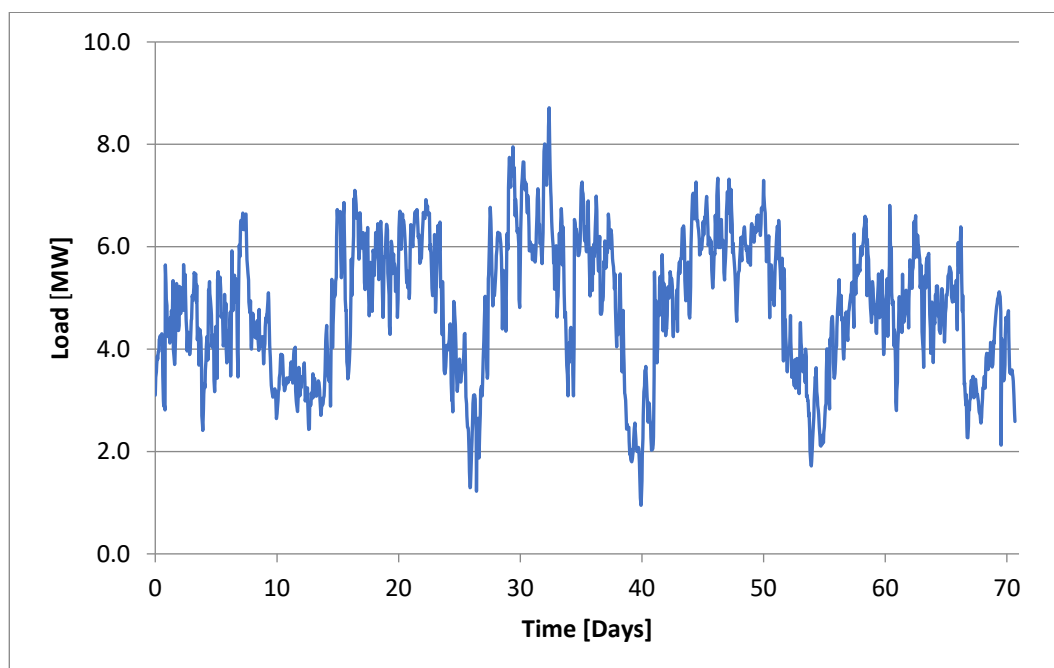


Figure 19: Validation input data, total cooling load

The maximum cooling load is well below the maximum AC chiller capacity as only the AHU units are simulated. FCU usually contribute by around 20-45 % of the total cooling load depending on weather conditions and other heat loads. The maximum capacity of the AHU circuit is around 11.5 MW so the capacity is well dimensioned for these time steps and location conditions.

Primary-chiller dedicated pumps were installed with enough capacity to overcome the pressure loss in the chiller at full load. Each primary pump was configured to always run with the corresponding chiller. The outgoing temperature from the chiller is constant and can be set differently for summer and winter conditions.

Each secondary circuit has its own set of pumps; the AHU circuit was equipped with three pumps. Two of the pumps have enough capacity to run the circuit at full capacity. The secondary pumps are controlled to run at a given pressure difference over the pumps. The pressure difference was set so that every consumer gets enough water at maximum load. The automation was designed so that the same number of pumps was running in the simulation as in the validation data to get at realistic secondary pump load.

The output settings were configured to give an output file with simulation time, pump load for all secondary pumps, number of running secondary pumps, total AC chiller load and total chilled water flow in the secondary circuit. The output was recorded every 10 minutes to give data points frequently enough.

The simulated pumping power was analyzed and compared with the actual validation data. The time period of 71 days was long enough to provide a good comparison, as it shows differences in day and night conditions as well as between early, mid and late summer. The output interval of 10 minutes was short enough to show some peaks that could be compared with the validation data. The output file consisted of 10 200 data points.

The relative error was used to compare the validation and simulated data, reporting the relative differences

$$\delta = \frac{\Delta x}{x},$$

where Δx is the absolute error and x is the actual validation data. The absolute error is

$$\Delta x = x_s - x,$$

where x_s is the simulated value. The cumulative relative error was also used to see the effect of the error over a longer time

$$\delta_{cum} = \frac{\sum \Delta x}{\sum x},$$

where $\sum \Delta x$ is the sum of absolute error over time and $\sum x$ is the sum of the validation data over time.

These indices give a view of the short-term and long-term simulation errors.

7.1. Validation results

The output of Apros is a text file that can be easily imported into Excel (Microsoft, 2010). Apros splits the data into columns according to output data. Apros has settings to configure the output file and column separator which is useful to further simplify the analysis of the data in other software.

Figure 20 compares the simulation data with the validation data. The simulation data is seen to follow the validation data quite well in general, but the real data shows larger peaks and the simulated results are smoother. The overall cumulative error is also quite small and reasonable.

The biggest deviation between simulated and real values can be found in the beginning of the simulation in the time interval 0-190 h. The deviation can easily be seen as the cumulative relative error is either rising or falling. The simulation is most accurate in the time interval 190-340 h as the cumulative relative error is not changing much. Other accurate intervals are 660-800 h and 1 150-1 250 h.

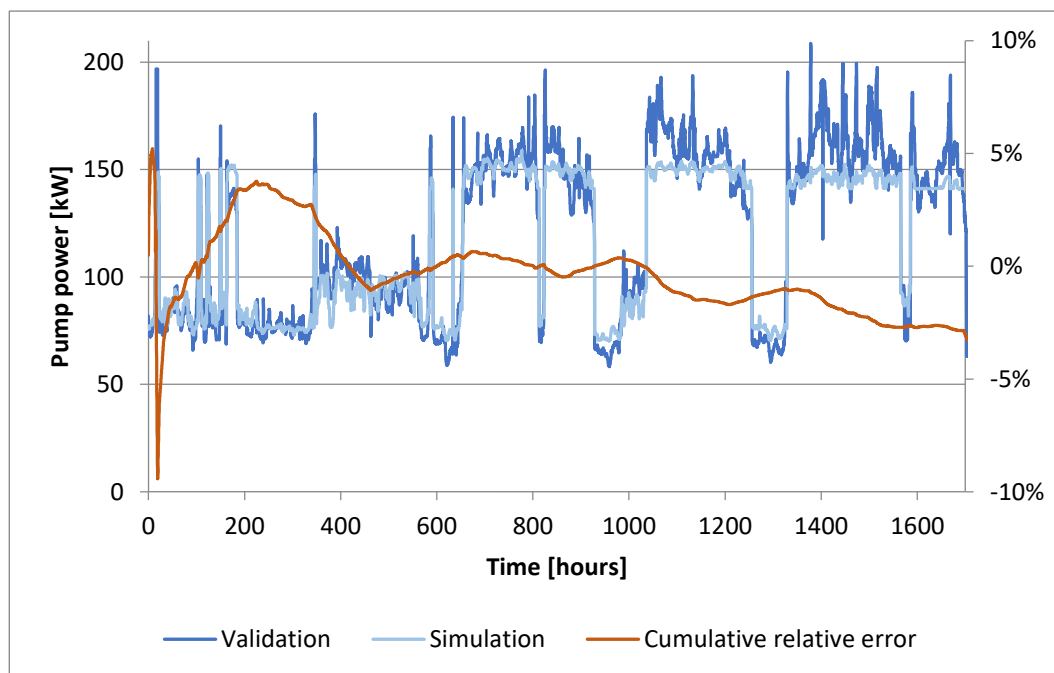


Figure 20: Comparison of secondary pumping power between simulation data and validation data

There are several peaks in the simulated data, where the pumping power is almost doubled in a short period of time. These peaks occur when the second pump is started. In the first third of the simulated period, the second pump is only running for short periods of time, i.e., a couple of hours at a time. In the latter two thirds, the second pump

is running almost constantly, with some occasional exceptions. The simulation seems to be more accurate for periods when two pumps are running. The use of two pumps in the latter two thirds of the period studied can be explained by the higher outdoor temperature.

The relative error is presented in Figure 21. Most errors are within $\pm 20\%$ with some peaks close to $\pm 30\%$. The average error is -1% .

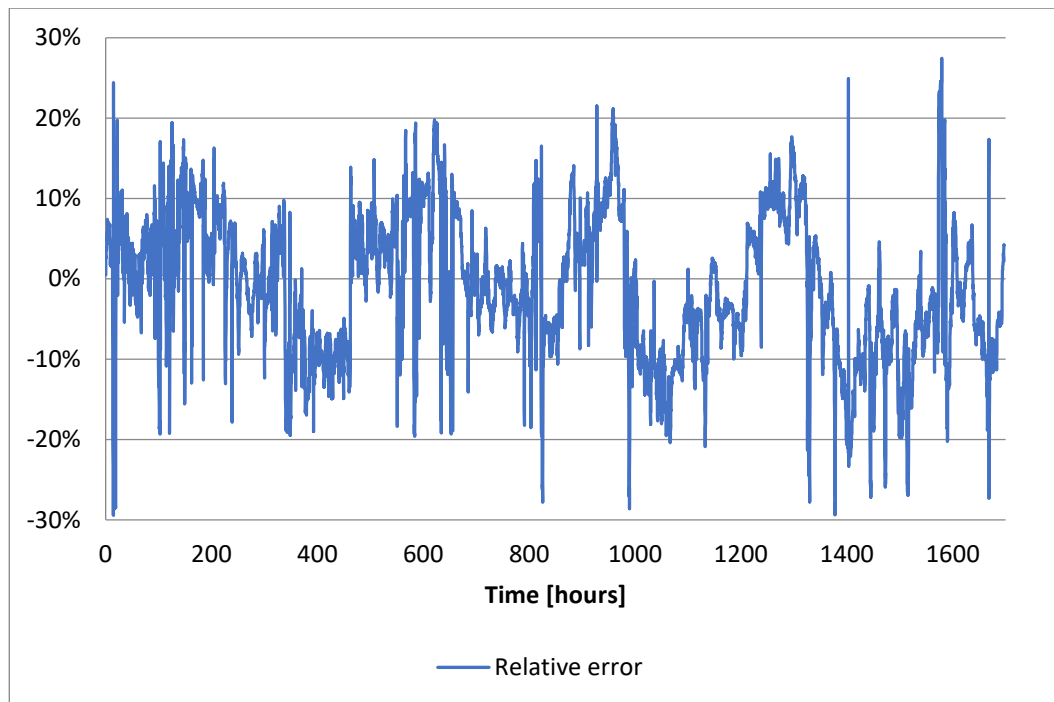


Figure 21: Relative error of simulation data compared to validation data

There are some larger errors in the simulation. One is in the beginning of the simulation, at 16-19 h. Analysis of the data shows a very large pumping power in the validation data. The surge lasts three and a half hours in the middle of the night, which might suggest some error in the data or pumps as the night load should be lower. Another large error occurs at 1 576-1 579 h when only one pump is running. The error seems to be low power consumption in the validation data as there is a change in the pump that is running. The error occurs for three hours and then abruptly drops from 25 % to 1 % in 10 minutes, which would suggest a data error.

The relative error is small overall and the average error is low. The errors are distributed quite equally on the positive and negative side, which has a positive effect on the overall error.

A histogram showing the distribution of the relative error is presented in Figure 22. The histogram is a good tool to show the individual relative errors' impact on the total error. The figure shows that a vast majority of the errors are within $\pm 10\%$, with the most common error at 0% . These small errors contribute to 84% of the total number of errors. Really large errors are few.

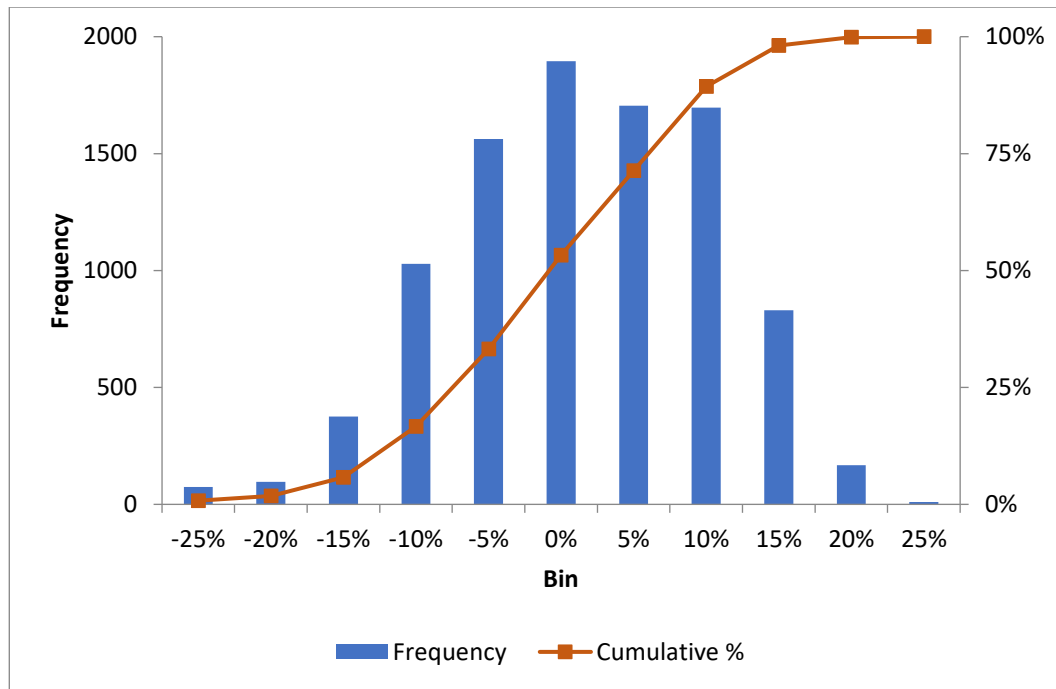


Figure 22: Histogram of the relative error, n = 9367

The simulation was done with a maximum time step of 0.5 s. This equals at least 14 million iterations, as Apros will shorten the time step if necessary. The simulation took around 9 h to run, which means that around 400 iterations were undertaken per second. Thus, the simulation is approximately 200 times faster than real time. This is a very tolerable simulation speed as it means that such simulations can be done overnight.

7.2. Conclusion of validation

The simulation results will never be completely accurate, as there have been simplifications made to the model. The cumulative relative error of -3% and an average relative error of -1% still confirm that the model is quite accurate. Figure 20 shows that the simulation follows the validation data in most cases, even though the validation data shows more spikes.

The key reasons for the deviation between validation and simulation data is that the simulation model is based on simplifications. Not every consumer is included and many

of the consumers are lumped to one. This leads to deviations as the simulated chilled water does not follow exactly the same path as in the real ship.

Another reason for errors is the limitations in the validation data. The time interval is one hour, which is quite a long interval. There are also limitations in the cooling load data as they are divided into big zones of consumers. The cooling load data was also only available for the AHU and not the FCU. All these limitations leave room for interpretations of the system, which leads to errors in the simulation.

Some larger errors were also found in the comparison between validation and simulation data. The pumps loads were either very low or very high, which would suggest that something is wrong either with the data logging or with the pumps.

The simplifications that were made during the model set up phase seem to be reasonable; the long-term simulation error was acceptable and the model is still sufficiently accurate for the design and decision phase of shipbuilding. For more accurate results, some more details and some sub-systems could be added.

The conclusion from the validation process is that Apros can handle simulation of the chilled water system. The validation confirms that the simulation tool and model work and that the output data is accurate enough for this study. Furthermore, the simulation speed is tolerable as Apros can do most simulations overnight.

8. Simulations

The simulations consist of a 41-day long cruise of the reference ship. All the pumping methods presented in Chapter 4 are simulated and compared, i.e., constant flow, constant primary - variable secondary flow and variable primary flow. This chapter presents the input data and the results from the simulations.

8.1. Input data

The input data was provided by the yard and was split into fire zones and type of spaces. The heat loads were provided as cooling needs expressed in kW. Some of the heat loads were combined and then set up according to fire zone and deck. Each fire zone and deck has its own input name in the simulation model and the data could be imported according to that. The input data used 5-minute intervals, but was for most parts calculated every hour.

The input data was calculated for the reference ship with variations according to outside enthalpy, solar gain, time of day, number of people in the space and heat loads from machines and appliances. The time span is 41 days and consists of cruises in the following areas: US east coast, the Caribbean, the Mediterranean, Asia and Australia.

Air-conditioning on-board cruise ships follows the international standard ISO 7547:2002. This ISO standard has guidelines on design condition and calculation of heat gain and losses as well as air-flow requirements. The standard provides procedures for calculation of maximum heat loads and design parameters, but the same equations are scalable to different conditions (ISO, 2002).

The standard sets an indoor temperature of 27 °C in summer and 22 °C in winter. Ship owners often have stricter requirements that are stated by the contract, often 22-24 °C. Relative humidity requirements for summer conditions are 50 % and at least 40 % of the supplied air should be fresh outdoor air. The maximum allowed persons in a space is also stated in the standard. These allowances are only for spaces that are not defined by the owner and they are listed in Table 4 (ISO, 2002).

Table 4: Maximum allowances in different spaces (ISO, 2002)

Space	Maximum allowance
Cabins	According to cabin accommodation design
Public spaces	In accordance to floor area: 1 person per 1.5 m ² for saloons 1 person per 2 m ² for dining areas 1 person per 5 m ² for recreation areas or the number of seats, e.g., theatre seats
Captain's and engineer's day-room	4 persons
Private day-rooms	3 persons
Hospital	Number of beds + 2
Gymnasium, game room	4 persons
First-aid room	2 persons
Offices	2 persons

These allowances can be used to approximate the number of persons in specific spaces throughout the day. The numbers of persons are needed in the calculations to get the necessary air flow and heat gain from persons.

The heat load of a person can be split into sensible heat and latent heat. Sensible heat is the heat that is perceived through a change in temperature and latent heat is the heat transferred without a change in temperature. The sensible heat depends on body activity and is approximated to 70 W for a body at rest and 85 W for a body at medium to heavy work. The latent heat is similarly approximated at 50 W for a body at rest and 150 W for a body at work. These values are for an indoor temperature of 27 °C and would be higher at lower indoor temperatures (ISO, 2002).

To calculate the heat transmission between adjacent spaces the equation

$$\phi = \Delta T [(k_v A_v) + (k_g A_g)],$$

is applied, where ΔT is the air temperature difference between the spaces [K], k_v is the heat transfer coefficient for surface v $\left[\frac{W}{m^2K}\right]$, A_v is the corresponding surface area [m²], k_g is the heat transfer coefficient for surface g $\left[\frac{W}{m^2K}\right]$, and A_g is the surface area of windows and scuttles [m²].

The temperature difference, ΔT , for the outside walls can be calculated if the outside temperature is known, as the indoor temperature is constant. Figure 23 shows the outside temperature on the 41-day reference cruise used in the simulations.

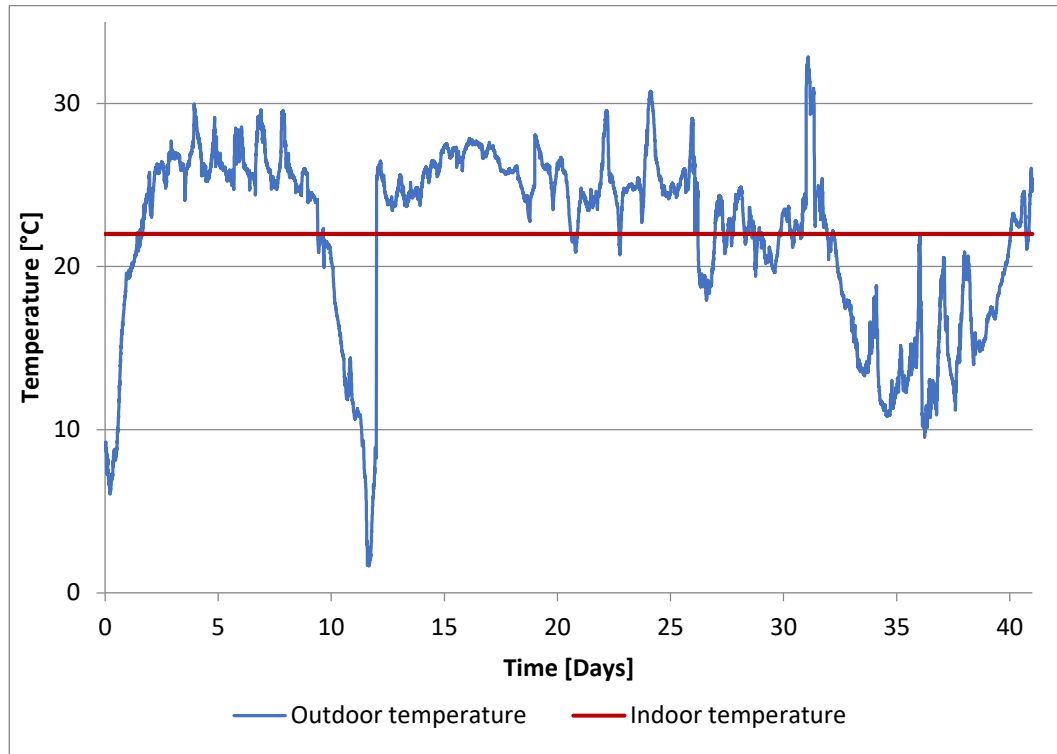


Figure 23: Outside temperature on 41-day reference itinerary

Cooling is needed to counteract heat transfer from outside when the outdoor temperature is higher than the indoor temperature. The cooling need is linearly dependent on the temperature difference. Analysis of the outdoor temperature shows that cooling is needed to combat outdoor heat transfer 60 % of the time.

Walls adjacent to some indoor spaces can also contribute to heat gain. Technical spaces such as engine rooms, boiler rooms and laundry are warmer than the rest of the ships and contribute to the heat gain. ISO 7547:2002 gives standard temperature differences to calculate the heat transfer from these spaces.

The heat transfer coefficient, k , is often found in the material specifications or as standard values in the ISO standard. The coefficient can be calculated by

$$\frac{1}{k} = \sum \frac{1}{\alpha} + \frac{\sum \frac{d}{\lambda} + M_L + M_b}{\mu},$$

where α is the heat transfer coefficient for the surface air $\left[\frac{W}{m^2K}\right]$, d is the thickness of material [m], λ is the thermal conductivity $\left[\frac{W}{m\cdot K}\right]$, M_L is the thermal insulance of the air gap $\left[\frac{m^2K}{W}\right]$, M_b is the thermal insulance of the different layers of material $\left[\frac{m^2K}{W}\right]$ and μ is the correction factor for the steel structure.

A typical heat transfer coefficient is $0.9 \frac{W}{m^2K}$ for an outside ship wall and between 3.5 and $6.5 \frac{W}{m^2K}$ for windows depending glazing (double or single). A smaller value signifies a better insulated surface.

Solar heat gain is dependent on sun intensity, surface angle in relation to the sun, color of surface and properties of the surface. A way to calculate the sun heat gain is by

$$\phi_s = \sum A_v k \Delta T_r + \sum A_g G_s,$$

where A_v is the sun exposed surface area [m²] (excluding windows), k is the heat transfer coefficient $\left[\frac{W}{m^2K}\right]$, ΔT_r is the additional temperature gained from the solar radiation, A_g is the area of the sun-exposed windows [m²] and G_s is the heat gain for the windows $\frac{W}{m^2}$.

There are also machines and appliances that contribute the heat gain other than heat gain from outside temperature, solar radiation and people. For example, galleys are a major contributor to the heat gain. The galley appliances use electricity and steam as energy sources and each appliance has a guideline on the amount of fresh air needed. Galley exhaust air can for most parts not be recirculated or used for enthalpy recovery as it is polluted with particles, smell and grease.

Lightning also contributes to the heat gain, but the heat gain is quite small per unit with modern LED light. Normal lamps have a power output of 15-40 W/m² depending on the lighting needs of the space. Fluorescent lights have a power output of 8-20 W/m², i.e., about half of a traditional lamp. LED lights have even lower power output for the same illumination.

Technical spaces, for example server rooms and electrical substations, have a very specific and predictable cooling need. These spaces have a constant cooling load and are not adjusted according to outside conditions.

It is not enough that the air conditioning maintains a suitable air temperature and humidity. The air flow to the spaces needs to be big enough so that the oxygen levels and

air freshness is maintained. The minimum air flow to a space is $8 \frac{1}{s}$ for every person the space is designed for. Some spaces, e.g., public restrooms, are regulated to have a set number of air changes per hour instead. The exhaust air for public restrooms needs to result in at least 15 air changes per hour.

The total heat load during the 41-day reference cruise is presented in Figure 24. A comparison of Figure 24 and Figure 23 shows a large dependence between total heat load and outside temperature. Furthermore, the time of day is seen as changes in heat load, from outside temperature and solar gain as well as people's activity.

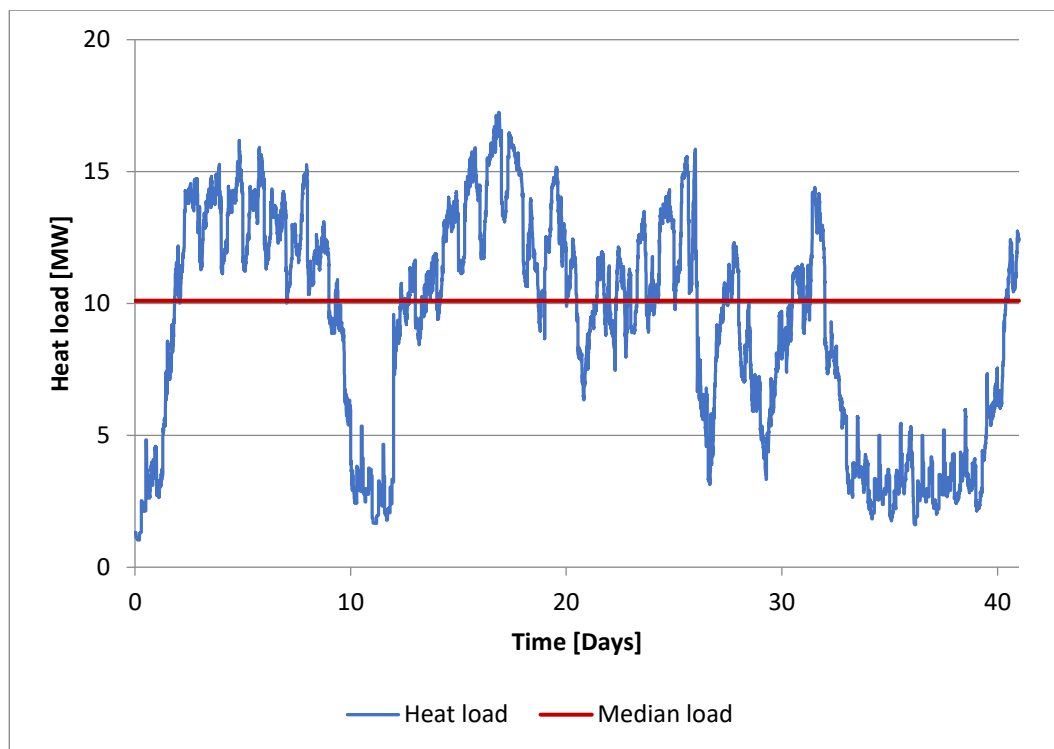


Figure 24: Total heat load for the reference cruise

8.2. Results

The following sections present the simulation results for each of the different pumping methods. An analysis and comparison of the results of the different methods are also provided. The comparison will focus on pumping method efficiency and return chilled water temperature.

8.2.1. Constant flow

Constant flow is the simplest configuration and expected to have very predictable results. There are two main pumps running at full power circulating the chilled water at a

constant speed. The water is pumped through all the chillers and the flow through the air handling unit is controlled by a three-way valve.

The results are presented in Figure 25 and are, as expected, a constant power usage with only minor variation (since the control loops have been designed appropriately). The flow is, likewise, stable at maximum capacity. It is apparent that the constant flow method wastes a lot of energy by pumping excess water through the whole system.

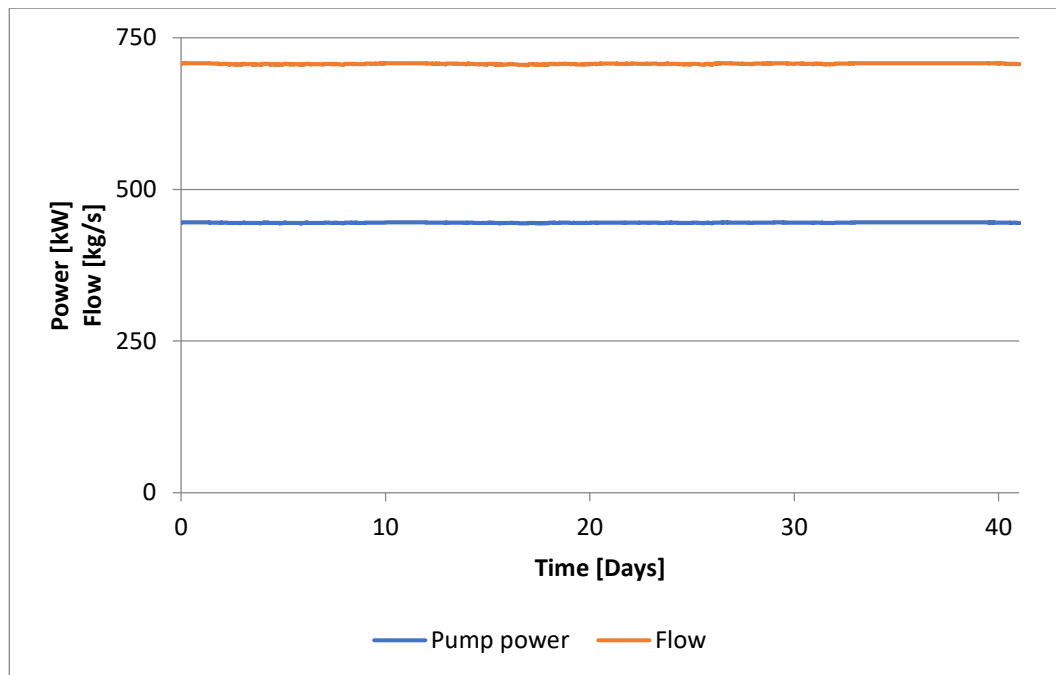


Figure 25: Pumping power and flow for constant flow method

The chillers' return chilled water temperature is changing according to load as the flow and supply temperature are constant. The return temperature is presented in Figure 26 and is at lowest just a fraction of a degree over the supply temperature. The highest temperature is close to the target temperature for the chiller, but it is still somewhat low.

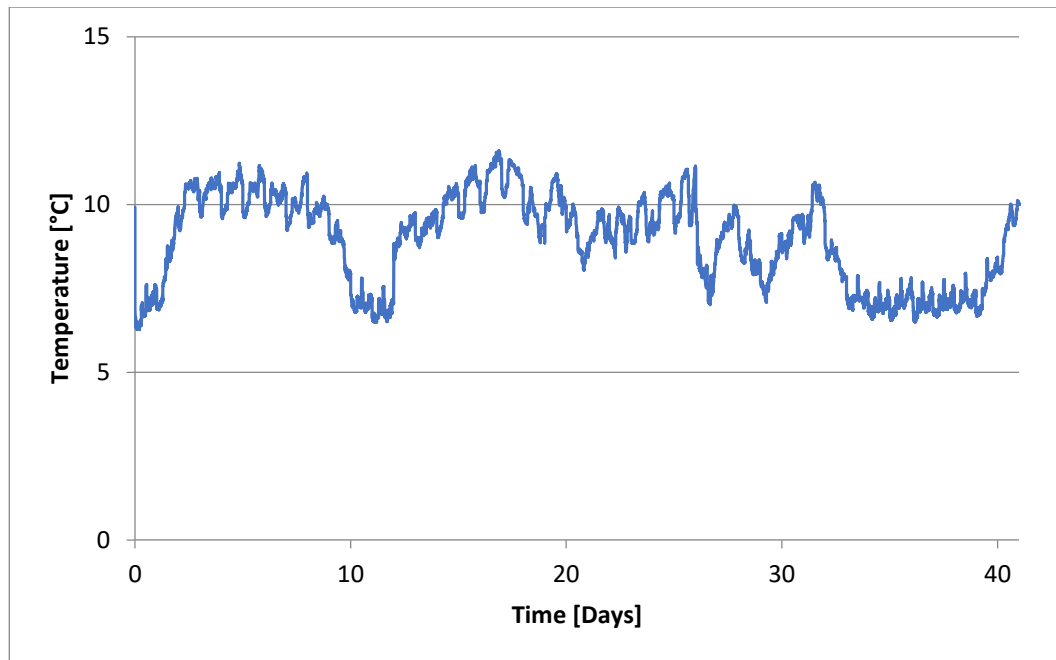


Figure 26: Chiller ingoing temperature for the constant flow method

8.2.2. Primary–secondary flow

The primary-secondary flow is much more complex and more difficult to predict. The constant primary pumps are always running synchronized with the chiller, so only the active chillers have water flowing through them. The secondary circuit pumps operate with a constant pressure difference. The temperature at the consumer is controlled with a standard two-way valve.

The results are presented in Figure 27 and the pump power is seen to have a lot more variation based on the load. The CWS flow depicted is the flow that goes through the consumers. There is still a large flow that is pumped unnecessary by the primary pumps, shown in the figure as decoupler flow. In some cases the decoupler flow is even larger than the actual CWS flow. There is clearly some room for improvement for a more efficient system design.

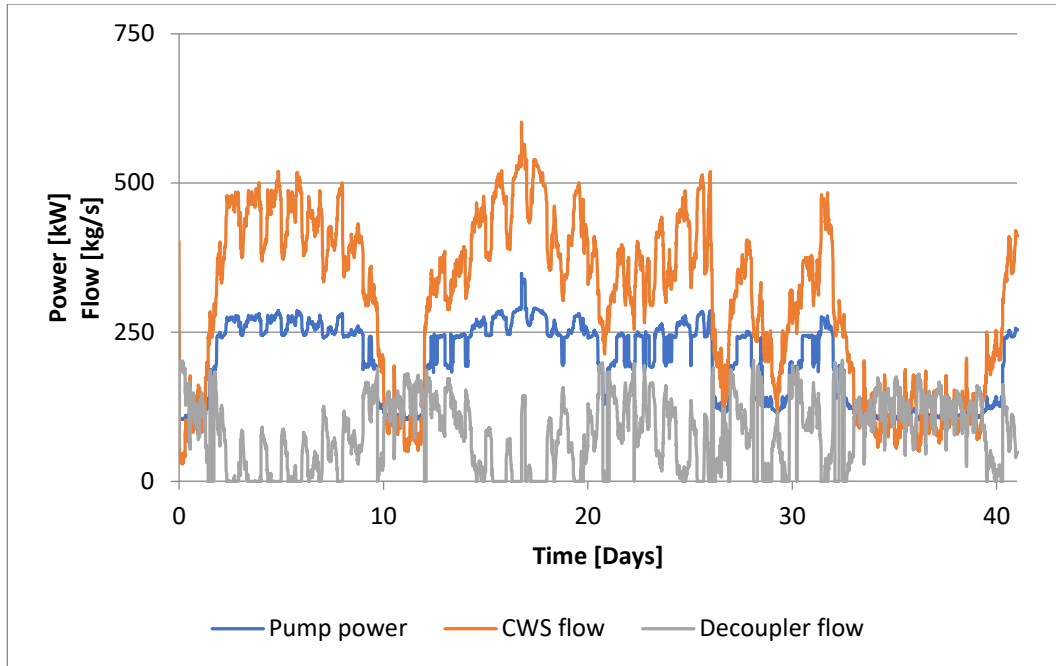


Figure 27: Pumping power and flows for primary-secondary flow method

The chillers’ return chilled water temperature is also in this case variable, even though the temperature shows less dependence on the conditions. The main return flow from the consumer has a stable temperature, but as it is mixed with the excess decoupler flow, the result is a lower return temperature to the chillers. The return temperature is presented in Figure 28 and is at its lowest only a little over the supply temperature, but is at higher load fairly close to the design return temperature.

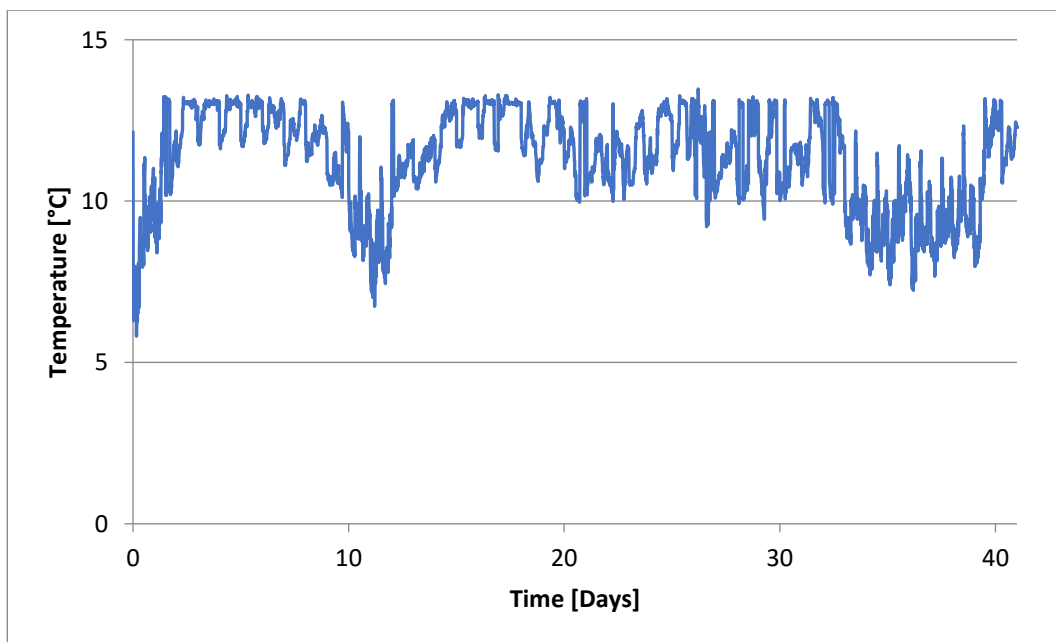


Figure 28: Chiller ingoing temperature for the primary-secondary flow method

8.2.3. Primary flow

The primary flow method should closely relate the flow to the heat load. The primary flow consists of a single circuit with a single set of pumps driven by a constant pressure difference. The consumer temperature is controlled with a standard two-way valve. A bypass valve is located close to the chillers to always guarantee at least a minimal flow through the chillers.

The results are presented in Figure 29. The pump power is, like in the primary-secondary method, very dependent on the heat load. The flow through the consumers is in direct relation to the heat load. A smaller bypass flow is still needed in colder climates when the heat load is small. The flow is, however, very small and only used to very limited extent.

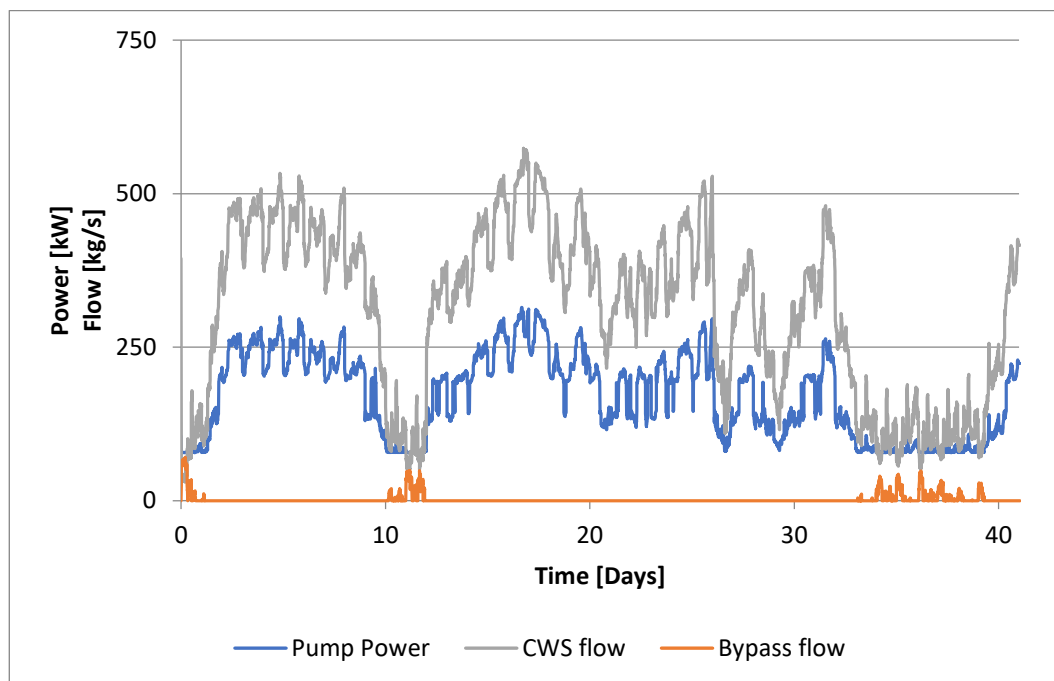


Figure 29: Pumping power and flows for the primary flow method

The return chilled water temperature for the chillers is much more stable in the primary flow method. There are still some smaller drops when the heat load is small and the bypass piping is used. The return temperature, presented in Figure 30, is even at its lowest point quite high. For most of the period studied, the return temperature is within a fraction of a degree from the design point.

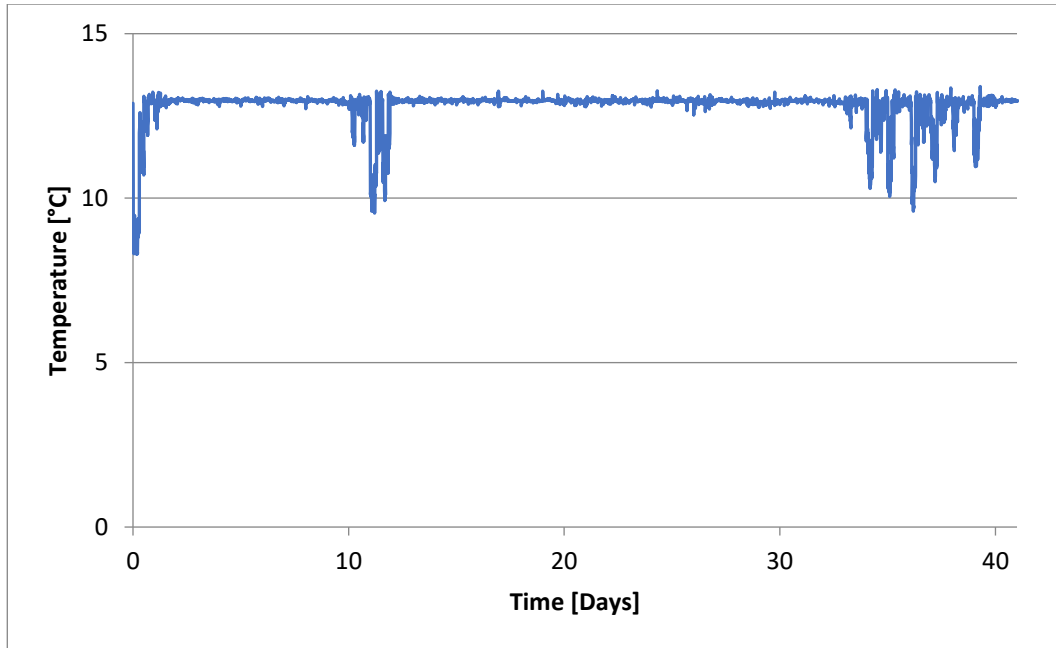


Figure 30: Chiller ingoing temperature with primary flow method

8.2.4. Comparing the results

The results seem to agree quite well with the expected outcome based on the literature surveyed in Chapter 2. The return chilled water temperatures varied a lot more in the methods with constant speed pumps and pumping power is lowest at the primary flow method.

Comparison of the pumping power for the entire 41-day reference cruise between the different cases gives the results presented in Table 5 and Table 6. Table 5 compares the cases with the constant flow case as the baseline, while Table 6 compares with the primary-secondary case as the baseline case.

Table 5: Comparison of pumping power of the cases with the constant flow case

Case	Expected savings	Simulation savings
Constant flow	0 %	0 %
Constant primary – Variable secondary	71 %	45 %
Primary flow	74 %	62 %

Table 6: Comparison of pumping power to primary-secondary flow case

Case			Expected savings	Simulation savings
Constant primary	–		0 %	0 %
Variable secondary				
Primary flow			11 %	15 %

The savings of primary flow compared to the constant flow case is a bit smaller than expected. This is mainly due to features of the reference cruise, with parts sailed in colder climate, yielding greater savings.

Both the constant primary and variable secondary methods perform worse than anticipated. This is likely due to the fact that the primary pumps pump a lot of excess water through the decoupler piping, thus wasting energy.

To get a better picture of the climate impact on the savings, the reference cruise is split into different itineraries based on location. The itineraries are, as mentioned earlier, the US east coast, the Caribbean, the Mediterranean, Asia and Australia.

Figure 31 presents the pumping power comparison on the 12-day reference itinerary from the US east coast. It is apparent that the savings are much larger at the lower temperatures in the northern parts of the US and smaller in the southern parts of the US.

Calculations show that the savings in pumping power comparing primary-secondary flow with constant flow is 53 % and from primary flow to constant flow 59 %. The savings comparing primary to primary-secondary flow is 13 %. The primary flow savings are a bit lower than the average as a large part of the cruise is in the southern hot climate. The primary-secondary method has larger savings here compared to the average. The primary flow is in these conditions the most efficient pumping method.

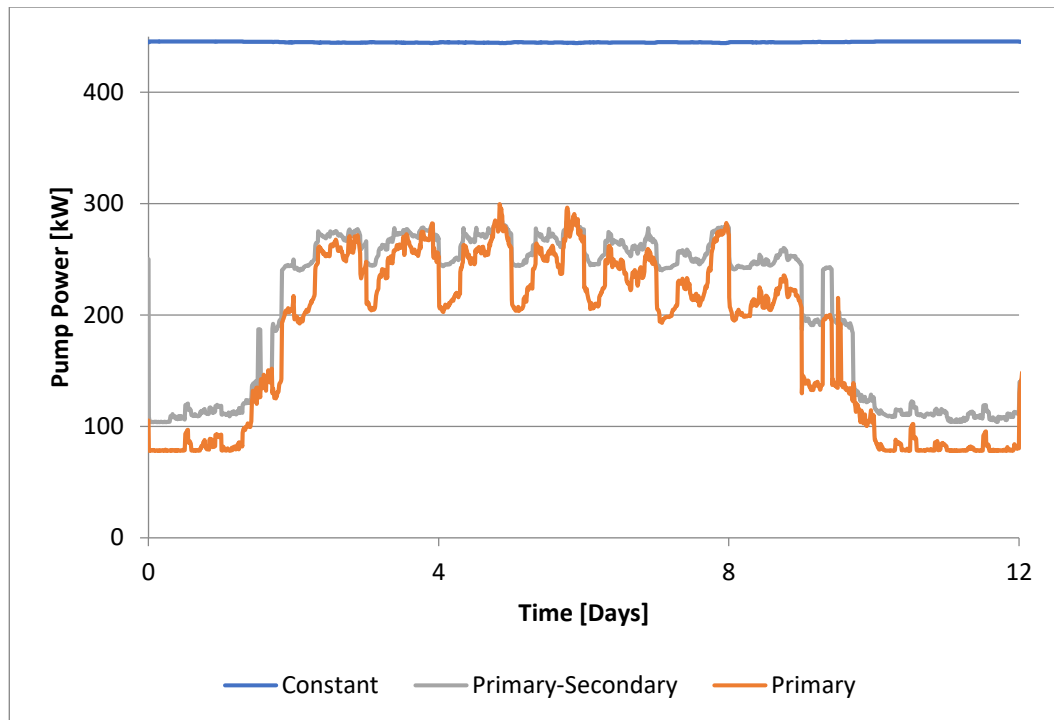


Figure 31: Pumping power on the US east coast cruise

A presentation of the pumping power for the different methods for the 7-day Caribbean reference itinerary is given in Figure 32. This part of the cruise contributes the least to the energy savings since the hot climate requires more overall pumping.

In some shorter time periods, e.g., around the 17th day, the pumping is even higher for the primary method than for the primary-secondary method. This is so because the primary constant pumps run quite efficiently when the load is high and all the water runs through to the consumers.

The primary method is still the most efficient method overall. The overall savings for the primary method is 49 % compared to the constant flow method and 11 % compared to the primary-secondary method. Comparing the primary-secondary flow method with the constant flow method shows savings of 43 %. The savings are more stable at the Caribbean cruise.

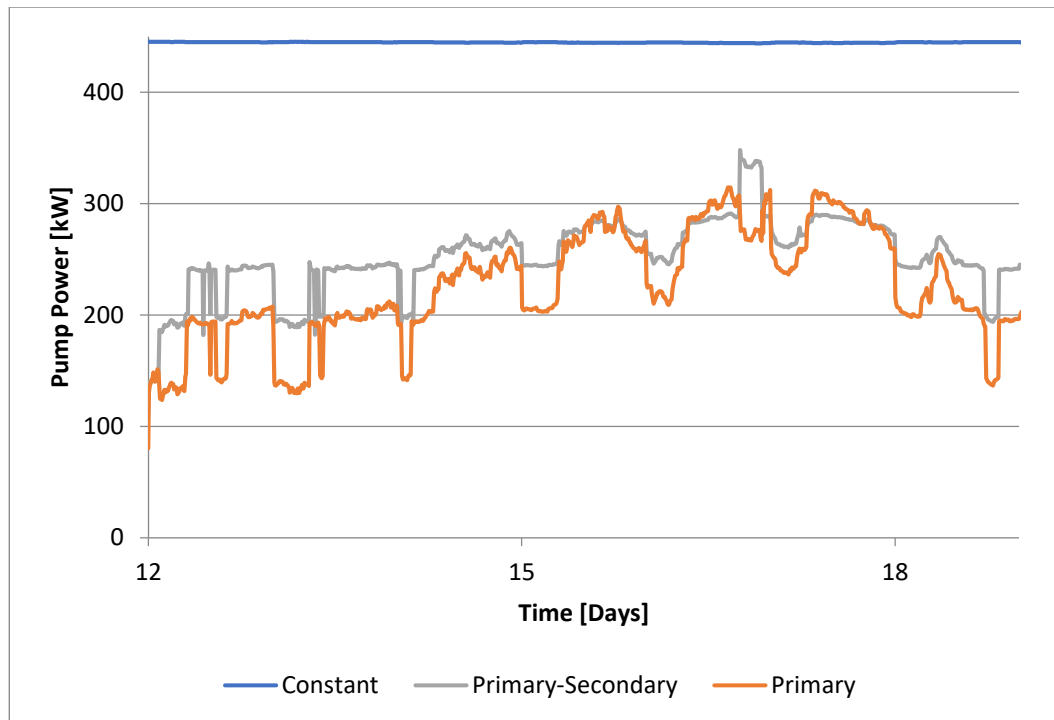


Figure 32: Pumping power on the Caribbean cruise

Figure 33 presents results from the 7-day Mediterranean reference itinerary. The somewhat cooler climate, compared to the Caribbean, offers more savings in pumping power. The primary method shows a quite stable energy saving compared to the primary-secondary setup under these conditions.

The different pumping methods also show similar results in these conditions. The primary-secondary setup is 47 % more efficient with respect to pumping power compared to constant method. The primary method saves 55 % in pumping power compared to constant flow and 15 % compared to the primary-secondary method and is therefore again the most efficient method.

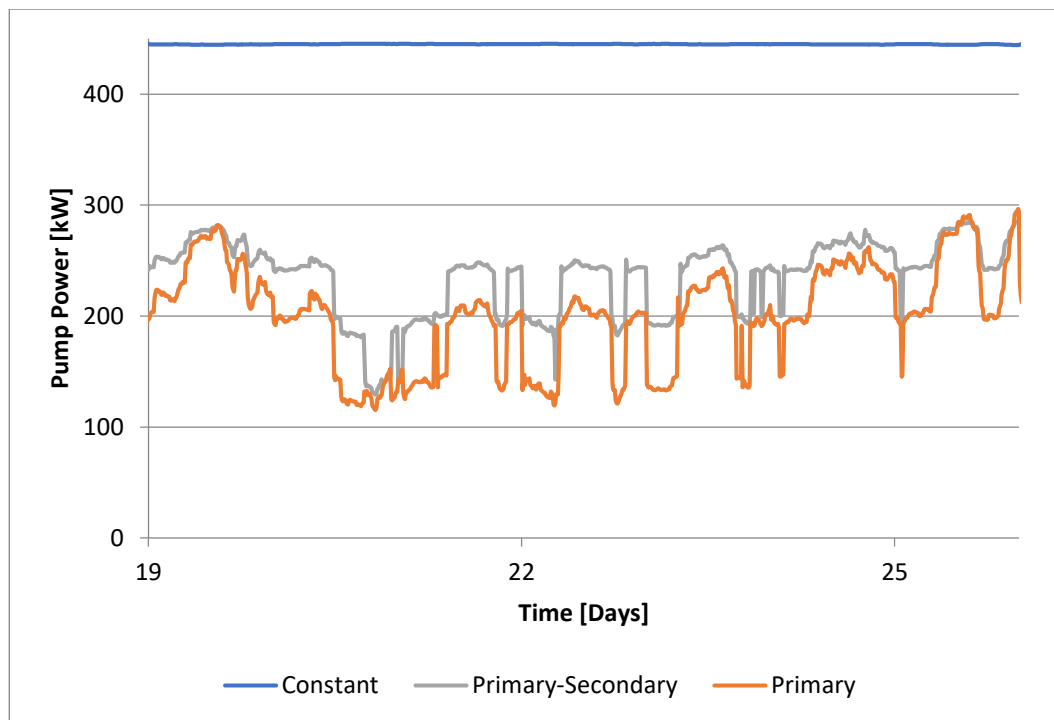


Figure 33: Pumping power on the Mediterranean cruise

In Figure 34 the pumping power results from the 5-day Asian reference itinerary are presented. The Asian reference cruise climate is quite variable. This shows up as short periods of higher pumping power.

Comparing the primary flow and primary-secondary flow, the savings are quite marginal until day 27 and for days 29-30, but the savings are more substantial in the other time periods. The pumping powers of the primary-secondary flow and the primary flow are overall quite low on this itinerary compared to the constant flow.

The primary-secondary method is 61 % more energy efficient than the constant method. The primary method is 68 % more energy efficient compared to constant method and 19 % more efficient compared to primary-secondary method.

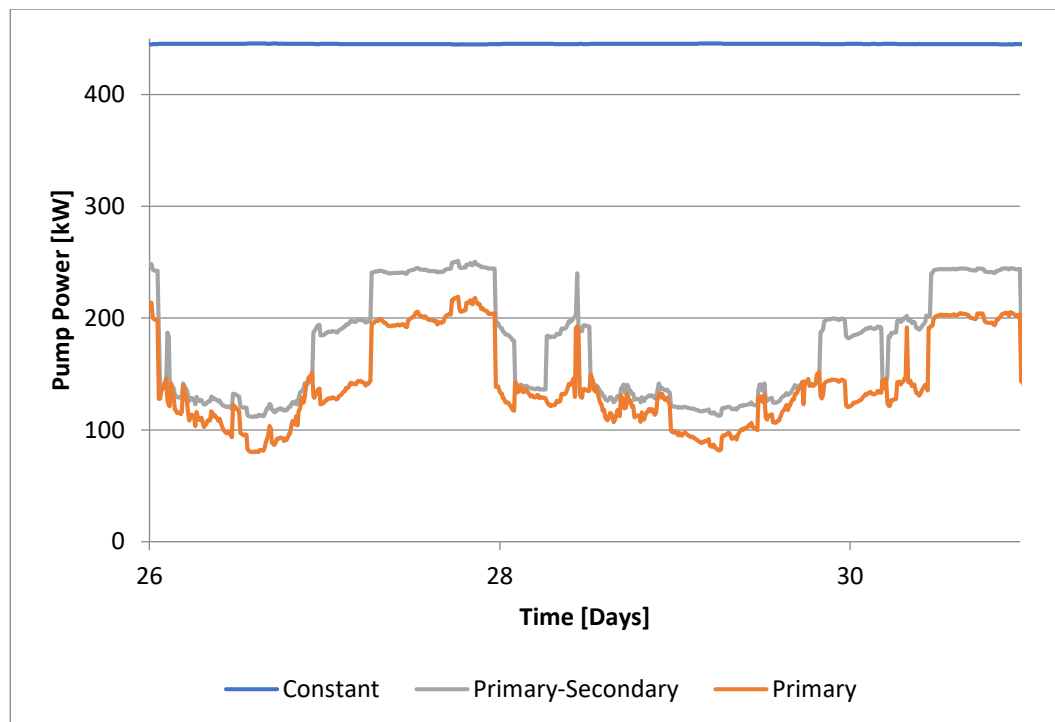


Figure 34: Pumping power on the Asian cruise

Finally, Figure 35 presents the pumping power for the last 10-day itinerary in Australia. The power consumption is low at this itinerary, similarly to the northern US part of the first itinerary.

This itinerary contributes to large savings especially compared to the baseline constant flow method. The primary-secondary method shows savings of 69 % compared to the constant flow setup. Similarly, the primary method shows savings of 75 % compared to constant flow and 21 % compared to primary-secondary method.

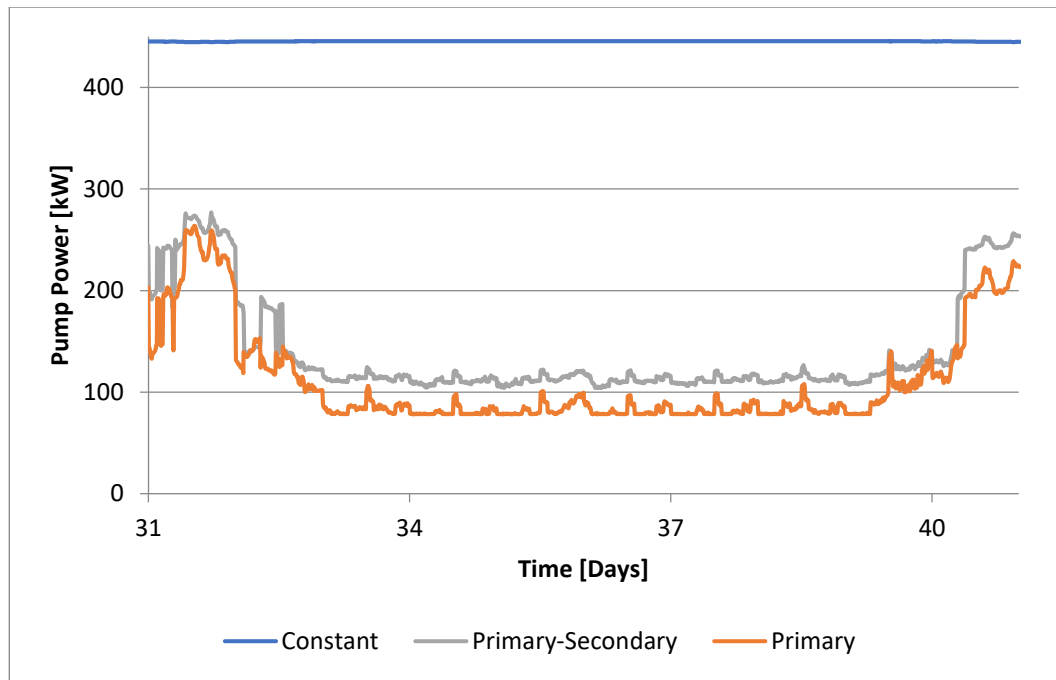


Figure 35: Pumping power on the Australian cruise

Comparing the return temperature to the chiller gives a similar result, where the more sophisticated methods perform closer to the design conditions. The primary flow method is very good at keeping the temperature close to chiller design values, with an exception for periods with very low heat loads. The constant flow performs poorly with return temperatures close to supply temperature in large parts of the reference cruise. The primary-secondary flow is acceptable for most part, but has problems especially at lower loads.

Table 7 presents an analysis of the return temperature, with focus on good values and too low values. With return temperatures less than 10 °C the temperature difference in the chiller is very small, which is bad for efficiency. A good return temperature is within half a degree of the optimal temperature.

Table 7: Comparison of return temperatures of the different pumping methods

Case	Return temperature less than 10 °C	Return temperature close to design temperature
Constant flow	75 %	0 %
Primary-secondary flow	20 %	39 %
Primary flow	1 %	94 %

9. Discussion

This chapter discusses the advantages and disadvantages of the different systems and compares them from an economical and technical viewpoint. The evaluations are based on the results of the simulations of Chapter 8. The price of electricity production onboard a cruise ship was approximated to be 100 €/MWh (Meyer, 2018).

The differences in investment cost for the different methods are quite small. The major parts of the system are similar, and the differences are particularly low between the constant flow and primary flow methods. The major differences between the constant flow and primary flow methods are the variable-frequency drives, which are not very expensive anymore. Another difference is a more advanced automation system for the primary flow method and replacing three-way valves with two-way valves. It is somewhat difficult to estimate the price of a more complex automation system. In conclusion, the investment cost for the primary-secondary system is the highest. There is a need for additional primary pumps as well as some additional piping, a more advanced automation system and variable-frequency drives. A rough estimate of additional investment costs over constant flow is 650 000 € for the primary-secondary method and 250 000 € for the primary flow method (Meyer, 2018). These are very gross estimates and especially the automation system part is difficult to price.

Assuming an installed pumping power of 445 kW, the 41-day reference cruise (cf. Chapter 8) gives significant savings with the alternative pumping methods. If the cruise ship is operating all year with no idle period, i.e., 8.9 cruises a year, the savings would be around 215 000 € for the primary-secondary method and around 240 000 € for the primary method. Comparing the primary method with the primary-secondary method gives savings of around 26 000 € a year, but also requires a smaller investment cost.

The savings vary quite considerably depending on the location of the cruise. The savings from different itineraries are presented in Figure 36. It is clear that the cooler the climate, the better the savings potential is, from as much as 292 000 € savings in Australia to 191 000 € in the Caribbean. The savings in Australia compared to the Caribbean are almost 53 % higher.

Even higher savings may be reached along with possible further savings in chiller power. Chiller power is expected to reduce as the chiller efficiency is higher when the return chilled water temperature is closer to the design value (Yu & Chan, 2008).

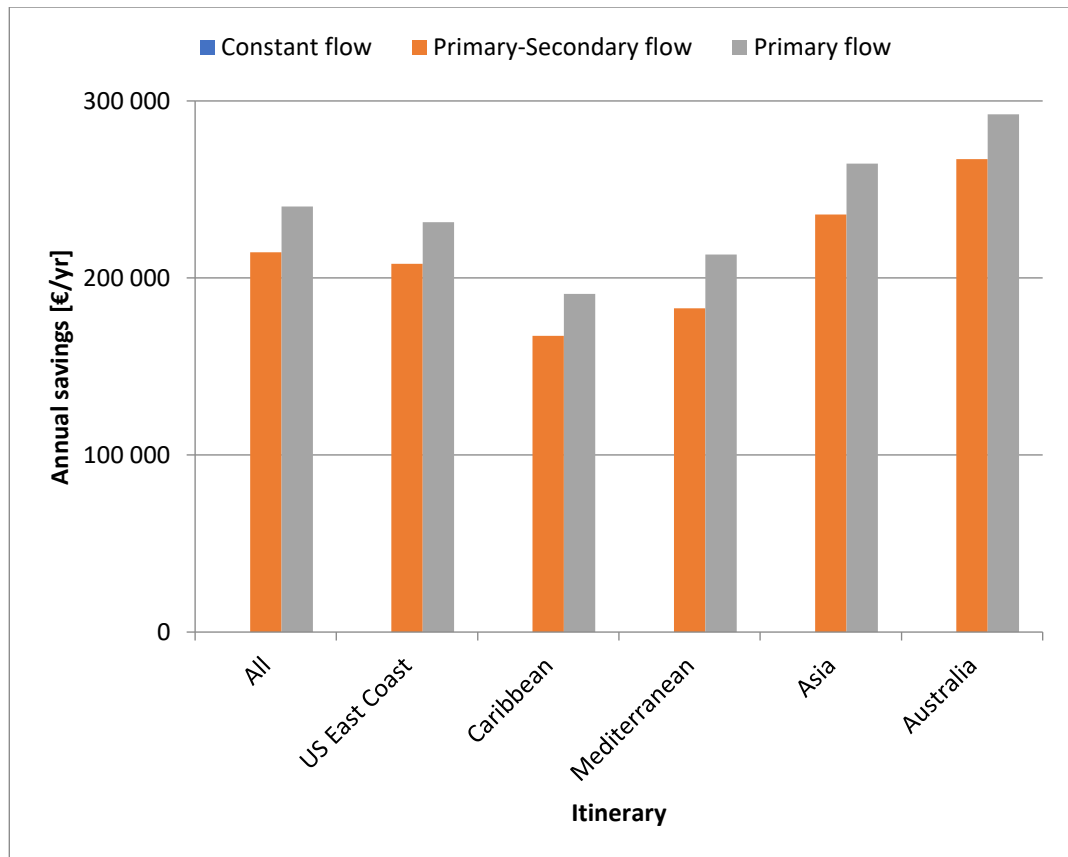


Figure 36: Annual savings for different itineraries

Comparing annual savings with investment costs gives the payback time. Payback time is the number of years for the investment to be profitable, i.e., the lower the better. The payback time is presented in Table 8. The payback time for the worst and best itinerary as well as a worst- and best-case scenario are also included. The worst-case scenario represents the worst itinerary as well as a 25 % drop in fuel prices. The best-case scenario, in turn, represents the best itinerary as well as a 25 % rise in fuel prices. A payback time of three years is usually considered good, and the payback time of the primary flow concept is almost half of that even in the worst-case scenario, which indicates that it clearly would be a very good investment.

Table 8: Payback time for the different pumping methods

Payback time [years]	Constant flow	Primary-Secondary flow	Primary flow
Average	0.00	3.03	1.04
Worst itinerary	0.00	3.88	1.31
Best itinerary	0.00	2.43	0.85
Best-case scenario	0.00	1.82	0.64
Worst-case scenario	0.00	4.85	1.64

There are some apparent advantages and disadvantages of each of the pumping methods that were observed in the simulation process. The constant flow method is very easy to control and has a low investment costs. There will always be enough flow and water in the system for all the AHU and FCU, but it is clearly very wasteful to have the pumps running at full speed all the time. The primary-secondary method will save power by having most of the pumping done by variable speed pumps. Still, the primary pumps run at full speed, but these are chiller specific and only run when the chiller is in use. The constant flow through the chiller makes the control easier, but the investment costs are the highest for this method.

The primary flow method will save most power with only one set of variable speed pumps running. The control is more difficult as the flow through the chiller is changing, but chiller efficiency will rise due to constant temperature difference over the chiller (Johnson Controls, 2018). The investment costs fall between those of the two other methods.

The overall results from the simulations and analysis are that the primary method is the most energy efficient and economical pumping method.

Some suggestions on how to further improve energy efficiency and how the accuracy of the simulation model could be enhanced is next discussed. There could be a saving potential in comparing the manifold versus dedicated pumping setup. Another interesting setup would be to drive the variable speed pumps with pressure differences varying according to load. To further improve the simulation accuracy, a more complex model could be built, i.e., with more consumers and a more accurate description of the piping network. There could also be improvements in the description of the action of the valves, pipes and heat exchangers to better replicate the real-life situation.

10. Conclusion

Tougher environmental requirements from both the International Maritime Organization and ship owners compel ship yards to develop more energy-efficient ships. HVAC account for roughly a third of the total power consumption of the ship hotel. Therefore, even relatively small savings in HVAC can contribute to a more energy efficient ship.

The objective of this thesis was to study and compare different pumping methods in the chilled water system to find possible savings. A comprehensive simulation model was built to validate these savings. The model was to be well documented and easily modifiable for further use. The simulation software used was Apros, which is an advanced dynamic simulation software tool developed by VTT and Fortum.

Three different pumping methods were studied and simulated. The methods studied are constant flow, primary-secondary flow and primary flow. Constant flow is the simplest method, where the pumps run at full speed all the time. The primary-secondary flow method has a primary circuit with constant chiller-specific pumping and a secondary circuit with variable speed pumps keeping a constant pressure difference. The primary flow concept consists of only variable speed pumps maintaining a constant pressure difference. All three methods are used in both land-based and maritime applications.

The simulation model was validated with data available from an existing cruise ship, as the reference ship for this thesis was not built yet. The validation ship was smaller than the reference ship, but used a relevant pumping method, the primary-secondary method, and the necessary data were available. The consumer heat load data were split across the ship to simulate the cooling needs. The results of the simulation were compared with the actual data available. The results were in general agreement with an overall average error of only -1 %. Therefore, the model was concluded to be accurate enough for the simulation purpose of the thesis.

The heat load for the simulations was calculated based on outside temperature, solar heat gain, people movement and appliances. The calculations were based on a 41-day reference cruise consisting of five different itineraries at the US east coast, the Caribbean, the Mediterranean, Asia and Australia. The total heat load varied between 1 MW and 17 MW.

The results from simulation of the different pumping methods showed that variable speed pumps could save a considerable amount of energy. The primary-secondary

method showed savings of 45 % over the constant flow methods, and the primary method showed 62 % savings. The primary flow system was 15 % more efficient than the primary-secondary flow system.

A more in-depth analysis of the results showed varying savings during different parts of the cruise. The hot and humid climate in the Caribbean required much more cooling, i.e. a larger chilled water flow. The larger flow cuts down savings, as the variable speed pumps ran at higher speed. The cooler climate on the Australian cruise had the lowest cooling needs and the savings were much higher under these conditions. Savings comparing the variable flow with the constant flow varied from 49 % at the Caribbean to 75 % at Australia.

The total savings in pumping power contribute to significant annual savings. The primary flow method saves on average 240 000 € a year compared to constant flow, while the primary-secondary method correspondingly saves 215 000 €. These savings are based on a power generation price of 100 €/MWh.

Another major benefit of the more complex pumping methods is a more stable return chilled water temperature. The constant pumping method yields a varying temperature difference over the chiller, especially for low loads. A return temperature below the design value will make the chiller less efficient. The primary-secondary method has a more stable return temperature, but it is still dependent on the load. The primary method keeps the return temperature to the chillers constant and very close to the design value. The return temperature only drops at very low loads.

The simulation results clearly show that the primary method is the most energy efficient and economical method, and that forthcoming ships should apply this design.

Svensk sammanfattning

Skeppsvarven är under ett ständigt ökat tryck att minska på utsläppen från kommande fartyg och öka energieffektiviteten. Dessa krav kommer både från internationella organisationer, såsom International Maritime Organization, och skeppsägarna. Oftast skall dessa förbättringar ske utan att minska på komforten eller upplevelsen för passagerarna ombord. Värme, ventilation och luftkonditionering (eng. HVAC) står för ungefär en tredjedel av elförbrukningen på kryssningsfartygens hotell vilket gör att inbesparingspotentialen är stor.

Syftet med detta diplomarbete var att undersöka luftkonditioneringens kylvattensystem och dess pumpningssystem för att hitta potentiella förbättringar. Dessutom skulle en simuleringsmodell byggas för att kunna bekräfta inbesparingspotentialen. Simuleringsmodellen skulle vara väldokumenterad och lätt att modifiera för eventuella bruk.

Pumpningsmetoderna som undersöktes var konstant flöde, primärt-sekundärt flöde och primärt flöde. Konstant flöde är den enklaste metoden som består av en krets vars pumpar körs med full effekt hela tiden. Primärt-sekundärt flöde består av ett primärflöde vars pumpar körs med full effekt och åtminstone ett sekundärt flöde där pumparna körs så att en konstant tryckskillnad upprätthålls i systemet. Primärpumparna är kylarspecifika och körs endast när kylaren används. Primärflöde är den mest avancerade metoden som består av en krets med pumpar som körs med konstant tryckskillnad.

Simuleringsmodellen byggdes i Apros, ett datorprogram för avancerad dynamisk simulering. Som bas för modellen fungerade ett framtida referensfartyg. För att validera modellen behövdes data från ett existerande fartyg. Valideringsfartyget var ett mindre fartyg där pumpningen av kylvattnet sker med primär-sekundärflödesmetoden. Fartyget var lämpligt då det var i ungefär rätt storleksklass, hade en relevant pumpningsmetod och det dessutom fanns tillräckligt noggranna data tillgängligt. Datat uppdelades i fartyget enligt typ av luftkylningsapparat och brandzon för att efterlikna det verkliga scenariot. Simuleringsresultatet jämfördes med verkliga data från valideringsfartyget. Avvikelsen mellan resultatet var överlag liten och medelavvikelsen låg på endast -1 %. Felet var tillräckligt litet för att modellen skall kunna användas för simuleringar av planerade skepp.

Som grund för simuleringarna behövdes en värmebelastning. Värmebelastningen räknades för varje del av fartyget, uppdelat i brandzoner och däck, utgående från utetemperatur och luftfuktighet, solstrålningen, passasernas rörelse i skeppet, belysning och apparater. Som grund för värmebelastningen användes en 41-dagars referenskrussning. Denna krussning består av fem olika rutter i USA:s östkust, Karibien, Medelhavet, Asien och Australien. De olika rutterna uppvisar stor variation på temperatur, luftfuktighet och solstrålning vilket gör det lämpligt för att beskriva olika tillstånd för fartyget. Den totala värmebelastningen varierade från 1 MW till dryga 17 MW.

Simuleringsresultatet från de olika pumpningsmetoderna visade att väsentliga mängder elektricitet kunde sparas om pumparnas hastighet kan regleras. Primärsekundärflödesmetoden skulle leda till en inbesparing på omkring 45 % jämfört med konstantflödesmetoden medan primärflödesmetoden skulle spara upptill 62 %. Primärflödesmetoden var således 15 % effektivare än primärsekundärflödesmetoden.

Vidare analys av resultaten gjordes för att klargöra hur mycket ruten påverkade energiförbrukningen. Karibiens heta och fuktiga klimat gjorde att kylningsbehovet var högre och pumparna gick på hög effekt. Denna rutt resulterade i den minsta inbesparingen. På den australienska ruten var klimatet mildare, vilket resulterade i det minsta kylnings- och pumpningsbehovet. Primärflödesmetoden besparing varierade från 49 % för den karibiska ruten till 75 % för den australienska ruten jämfört med konstantflödesmetoden.

De mer avancerade pumpningsmetoderna bidrar till betydande årliga kostnadsbesparingar. Primärt flöde sparar i medeltal 240 000 € jämfört med konstant flöde och primärt-sekundärt flöde sparar på motsvarande sätt 215 000 €. Inbesparingen mellan primärt flöde och primärsekundärt flöde är 25 000 €. Dessa beräkningar baserar sig på ett elproduktionspris på 100 €/MWh.

Dessa kostnadsbesparingar kan jämföras med investeringskostnaderna för att kunna bestämma återbetalningstiden. Återbetalningstiden för primärt flöde är 1.04 år för hela referenskrussningen och för primärsekundärt flöde 3.03 år. Även ett värsta fall och bästa fall analyserades. Det värsta fallet bestod av ruten som sparade in minst pumpningseffekt och där priset på bränsle sjunkit med 25 %. Det bästa fallet bestod av ruten med högsta inbesparingen i pumpningseffekt och där priset på bränsle stigit med 25 %. Dessa fall gav en återbetalningstid för primärt flöde på 1.64 år för det värsta fallet

och 0.64 år för det bästa fallet. Speciellt för primärflödesmetoden är återbetalningstiden väldigt kort, även i det värsta fallet, vilket indikerar att det vore en mycket god investering.

En annan fördel med de mer komplexa pumpningsmetoderna är effekten på temperaturen för returvattenflödet till kylarna. Ett konstant flöde gör att returtemperaturen varierar kraftigt med värmebelastningen. Primärt-sekundärt flöde klarar av att hålla returtemperaturen aningen högre men den varierar ändå med värmebelastningen. Primärt flöde klarar av att hålla en nästan konstant returtemperatur, med undantag för perioder med väldigt låga värmebelastningar. En jämn returtemperatur nära kylarens designtemperatur bidrar till en effektivare kylning.

Simuleringsresultatet indikerar att primärflödesmetoden skulle vara den mest energieffektiva samt den mest ekonomiskt lönsamma. Även primär-sekundärflödesmetoden har god ekonomisk lönsamhet men den större investeringskostnaden är inte motiverad då det finns en billigare och effektivare metod.

References

- Abouelkawam, M. 2017, *Seafarers and Energy Efficient ships: One step Ahead* [Homepage of World Maritime University Malmö], [Online]. Available: https://commons.wmu.se/cgi/viewcontent.cgi?referer=https://www.google.fi/&httpsredir=1&article=1042&context=marener_conference [2018, 11/5].
- AGA industrigaser 2018, *R134a* [Homepage of AGA industrigaser], [Online]. Available: http://www.aga.se/sv/products_ren/refrigerants/hfc_gases/r134a/index.html [2018, 18/05].
- Aittomäki, A. (ed) 2012, *Kylmäteknikka*, 4th edn, Bookwell Oy, Finland.
- Apros 2018, *Apros Process Simulation Software* [Homepage of Apros], [Online]. Available: <http://www.apros.fi/en> [2018, 11/05].
- Arora, R.C. 2012, *Refrigeration and air conditioning*, 3rd edn, PHI Learning Pvt. Ltd, New Delhi.
- ASHRAE 1996, *ASHRAE Handbook: HVAC systems and equipment*, 1st edn, American Society of Heating, Refrigerating, and Air Conditioning Engineers, Atlanta, GA.
- Aspen Tech 2018, *Aspen Plus* [Homepage of Aspen Plus], [Online]. Available: <https://www.aspentech.com/en/products/engineering/aspen-plus> [2018, 09/19].
- Bahnfleth, W.P. & Peyer, E. 2001, "Comperative Analysis of Variable and Constant Primary-Flow Chilled-Water-Plant Performance", *HPAC Engineering*, [Online], pp. 08/06. Available from: <https://pdfs.semanticscholar.org/3a0f/889cf6c4d78033522a5d7091e6a1013de3b6.pdf>. [8/6/2018].
- Barton, P. 1997, *Industrial experience with dynamic simulation*, Massachusetts Institute of Technology, Cambridge.
- Cao, T., Lee, H., Hwang, Y., Radermacher, R. & Chun, H. 2015, "Performance investigation of engine waste heat powered absorption cycle cooling system for shipboard applications", *Applied Thermal Engineering*, vol. 90, no. 1359-4311, pp. 820-830.

Carnival Corporation 2018, *Corporate Information* [Homepage of Carinival Corporation], [Online]. Available: <http://phx.corporate-ir.net/phoenix.zhtml?c=200767&p=irol-prlanding> [2018, 08/19].

Carnival Corporation 2018, *Green ship design, operations & maintenance* [Homepage of Carnival Corporation], [Online]. Available: <http://phx.corporate-ir.net/phoenix.zhtml?c=140690&p=irol-sustainability> [2018, 09/19].

Central-Air-Conditioner-and-Refrigeration.com, How does basic refrigeration cycle work?, [Online]. Available: <http://www.central-air-conditioner-and-refrigeration.com/basic-refrigeration-cycle.html> [2018, 11/07]

Chegg Study, *Psychrometric chart*. Available: <https://www.chegg.com/homework-help/questions-and-answers/cold-air-10c-dry-bulb-temperature-5c-wet-bulb-temperature-mixed-warm-moist-air-25c-dry-bul-q4960406> [2018, 08/19].

CLIA 2018, *2018 Cruise Industry Outlook*, Cruise Lines International Association, USA.

European Commission 2018, *Reducing emissions from the shipping sector* [Homepage of European Commission], [Online]. Available: https://ec.europa.eu/clima/policies/transport/shipping_en [2018, 08/23].

Fang, L., Clausen, G. & Fanger, P.O. 1998, "Impact of temperature and humidity on the perception of indoor air quality", *Indoor air*, vol. 8, no. 2, pp. 80-90.

Goldman Energy, *Double effect exhaust gas driven absorption chiller* [Homepage of Goldman Energy], [Online]. Available: <http://goldman.com.au/energy/company-news/how-does-an-absorption-chiller-work/> [2018, 05/17].

Hakala, T. 2012, *Calculation tool for fan coil unit*, Master's thesis, Tampere University of Technology, Tampere.

Horuz, I. 1998, "A comparison between ammonia-water and water-lithium bromide solutions in vapor absorption refrigeration systems", *International Communications in Heat and Mass Transfer*, vol. 25, no. 5, pp. 711-721.

IMO 2018a, *Air Pollution, Energy Efficiency and Greenhouse Gas Emissions* [Homepage of International Maritime Organization], [Online]. Available: <http://www.imo.org/en/OurWork/Environment/PollutionPrevention/AirPollution/Pages/Default.aspx> [2018, 10/15].

IMO 2018b, *Energy Efficiency Measures* [Homepage of International Maritime Organization], [Online]. Available: <http://www.imo.org/en/OurWork/Environment/PollutionPrevention/AirPollution/Pages/Technical-and-Operational-Measures.aspx> [2018, 10/17].

IMO 2014, *2014 Guidelines on survey and certification of the energy efficiency design index (EEDI)*, International Maritime Organization, London.

IMO 2013a, *2013 guidelines for calculation of reference lines for use with the energy efficiency design index (EEDI) for cruise passenger ships having non-conventional propulsion*, International Maritime Organization, London.

IMO 2013b, *Marine environment protection committee: Air pollution and energy efficiency. Energy efficiency for cruise passenger ships.*, International Maritime Organization, London.

IMO 2011, *IMO and the Environment*, International Maritime Organization, London.

ISO 2002, *Ships and marine technology - Air-conditioning and ventilation of accommodation spaces - Design conditions and basis of calculations (ISO 7547:2002)*, International Standard Organization.

Johnson Controls 2018, *E-mail correspondence with Johnson Controls*.

Johnson Controls 2017, *Benefits of Variable Primary Flow* [Homepage of Johnson Controls], [Online]. Available: <https://www.youtube.com/watch?v=41jRD61MW1o> [2018, 08/23].

Kirsner, W. 1996, "Chilled water plant design", *HEATING PIPING AND AIR CONDITIONING-CHICAGO-*, vol. 68, pp. 73-80.

Lappalainen, J., Blom, H. & Juslin, K. 2012, "Dynamic process simulation as an engineering tool – A case of analysing a coal plant evaporator", *VGB Powertech*, vol. 92, no. 1-2/2012, pp. 62-68.

Lee, K. & Cheng, T. 2012, "A simulation–optimization approach for energy efficiency of chilled water system", *Energy and Buildings*, vol. 54, pp. 290-296.

Lepistö, V., Lappalainen, J., Sillanpää, K. & Ahtila, P. 2016, "Dynamic process simulation promotes energy efficient ship design", *Ocean Engineering*, vol. 111, pp. 43-55.

Lepistö, V., Lappalainen, J., Sillanpää, K. & Ahtila, P. 2015, "Use of a commercial dynamic process simulator to enhance energy efficient ship design", Green Ship Technology Conference GST Copenhagen, Denmark, Copenhagen, Denmark, 11/03/15 - 12/03/15.

Madison gas and electric 2015, *Reheat systems for commercial buildings* [Homepage of Madison gas and electric], [Online]. Available: <https://www.mge.com/images/PDF/Brochures/business/ReheatSystemForCommercialBuildingsFactSheet.pdf> [2018, 06/12].

MathWorks 2018, *Simulink* [Homepage of Mathworks], [Online]. Available: https://se.mathworks.com/products/simulink.html?s_cid=wiki_simulink_2 [2018, 06/12].

Meyer 2018, *Various internal documents*, Turku, Finland.

Microsoft 2010, *Microsoft Excel 2010 Version 14.0.7212.5000*, 2010th edn, Microsoft.

Motorship 2018, *ECKERÖ LINE SAVES FUEL WITH ABSORPTION COOLER* [Homepage of Motorship], [Online]. Available: <https://www.motorship.com/news101/ships-equipment/eckero-line-saves-fuel-with-absorption-cooler> [2018, 5/24].

Nesbitt, B. 2006, *Handbook of Pumps and Pumping*, 1st edn, Elsevier Science Ltd, Newcastle, UK.

Nurmi, M. 2017, *Improving the energy efficiency of a cruise ship stateroom*, Master's thesis, Aalto University, Espoo.

RCCL 2018, *Interactive Analyst Center* [Homepage of Indigo tools], [Online]. Available: <http://apps.indigotools.com/IR/IAC/?Ticker=RCL&Exchange=NYSE> [2018, 07/20].

RCCL 2017, *Sustainability report* [Homepage of Royal Caribbean Cruise Line], [Online]. Available: <http://sustainability.rclcorporate.com/> [2018, 07/20].

Saiver, *Heat Recovery Units* [Homepage of Saiver], [Online]. Available: <http://www.saiver.com/en/heat-recovery-units-commercial/> [2018, 07/20].

Swedegas 2018, *Fakta om LNG* [Homepage of Swedegas], [Online]. Available: https://www.swedegas.se/gas/LNG/fakta_om_lng [2018, 05/23].

Taylor, S.T. 2002, "Primary-only vs. primary-secondary variable flow systems", *ASHRAE Journal*, vol. 44, no. 2, pp. 25-29.

Thermax 2018, *HOT WATER DRIVEN CHILLERS* [Homepage of Thermax], [Online].

Available from: <https://www.thermaxglobal.com/thermax-absorption-cooling-systems/vapour-absorption-machines/hot-water-driven-chillers/>; [2018, 5/24].

Tirmizi, S.A., Gandhidasan, P. & Zubair, S.M. 2012, "Performance analysis of a chilled water system with various pumping schemes", *Applied Energy*, vol. 100, pp. 238-248.

Trane 2011, *Applications Engineering Manual: Chiller System Design and Control*, [Online]. Available from: <http://www.tranebelgium.com/files/book-doc/12/fr/12.1hp13yp1.pdf> [2018, 06/12].

Tuuri, S. & Paljakka, M. "Apros Datasheet Thermal Hydraulics Modelling", [Online].

Available from: http://www.apros.fi/filebank/209-Apros_Datasheet_Thermal_Hydraulics_Modelling.pdf [2018, 07/20].

Ukkonen, A. 2018, *Advanced LNG cryogenic energy recovery in a modern cruise ship*, Master's thesis, Tampere University of Technology, Tampere.

Viking Line 2018, *Viking Linen ympäristötyö*. [Online], Available from:

<https://www.youtube.com/watch?v=kl-mr5FZXEI> [2018, 07/20]

Wang, S.K. 2001, *Handbook of refrigeration and air conditioning*, 1st edn, McGraw-Hill, New York.

Westerlund, T. 2009, *Anläggnings- och systemteknik*, Department of Chemical Engineering, Turku.

Ylijoki, J., Karppinen, I., Puska, E. & Silde, A. 2015, *Apros validation Selected cases related to nuclear safety analyses and training simulations*, [Online], Available from:

http://www.apros.fi/filebank/189-Validation_cases_list.pdf [2018, 09/19].

Yu, F. & Chan, K. 2008, "Improved energy performance of air cooled centrifugal chillers with variable chilled water flow", *Energy conversion and management*, vol. 49, no. 6, pp. 1595-1611.

Figures

Figure 1: Reference EEDI for different cruise ship sizes, year 2010 and 2025	4
Figure 2: RCCL fuel costs during the years 2015-2017 (RCCL, 2018).....	6
Figure 3: Pumping power dependency on ambient temperature (Tirmizi et al., 2012) ...	7
Figure 4: Psychrometric chart of humid air (Chegg Study)	12
Figure 5: Electric compressor chiller working principle (Central-Air-Conditioner-and-Refrigeration.com)	13
Figure 6: LNG phase diagram (ISO, 2015).....	16
Figure 7: Absorption chiller principles (Goldman Energy)	17
Figure 8: Air handling unit with enthalpy recovery wheel (Saiver).....	19
Figure 9: Fan coil unit (Hakala, 2012)	21
Figure 10: Constant flow pumping method	24
Figure 11: Constant primary - Variable secondary pumping method	25
Figure 12: Variable flow method	26
Figure 13: Dedicated pumps.....	27
Figure 14: Manifold pumps	28
Figure 15: Example of Apros 6 process diagram	30
Figure 16: Example of Apros 6 automation diagram.....	30
Figure 17: Automation of the consumer valve.....	35
Figure 18: Automation of the chillers.....	35
Figure 19: Validation input data, total cooling load	38
Figure 20: Comparison of secondary pumping power between simulation data and validation data	40
Figure 21: Relative error of simulation data compared to validation data.....	41
Figure 22: Histogram of the relative error, n = 9367	42
Figure 23: Outside temperature on 41-day reference itinerary	46
Figure 24: Total heat load for the reference cruise	48
Figure 25: Pumping power and flow for constant flow method	49
Figure 26: Chiller ingoing temperature for the constant flow method.....	50
Figure 27: Pumping power and flows for primary-secondary flow method	51
Figure 28: Chiller ingoing temperature for the primary-secondary flow method	51
Figure 29: Pumping power and flows for the primary flow method.....	52
Figure 30: Chiller ingoing temperature with primary flow method.....	53
Figure 31: Pumping power on the US east coast cruise	55

Figure 32: Pumping power on the Caribbean cruise	56
Figure 33: Pumping power on the Mediterranean cruise	57
Figure 34: Pumping power on the Asian cruise.....	58
Figure 35: Pumping power on the Australian cruise	59
Figure 36: Annual savings for different itineraries.....	61

Tables

Table 1: Average CWS load for the validation ship	9
Table 2: Potential savings in pumping power in the different cases	9
Table 3: Comparison between reference and validation ship	37
Table 4: Maximum allowances in different spaces (ISO, 2002)	45
Table 5: Comparison of pumping power of the cases with the constant flow case.	53
Table 6: Comparison of pumping power to primary-secondary flow case	54
Table 7: Comparison of return temperatures of the different pumping methods.....	59
Table 8: Payback time for the different pumping methods	62